BioMed Research International

New Prognostic and Predictive Markers in Head and Neck Tumors

Guest Editors: Monica Cantile, Francesco Longo, and Franco Fulciniti

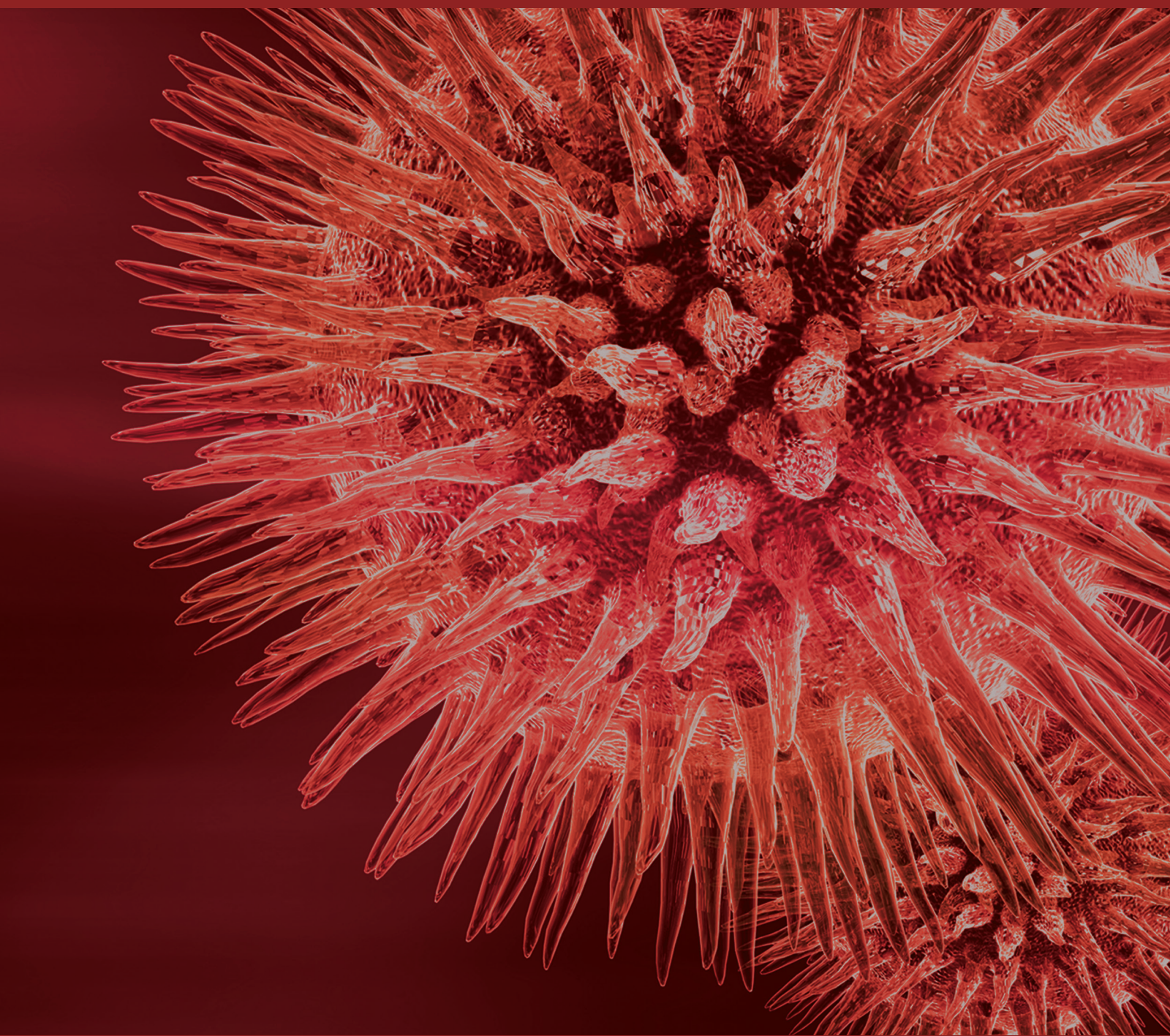

New Prognostic and Predictive Markers in Head and Neck Tumors

BioMed Research International

New Prognostic and Predictive Markers in Head and Neck Tumors

Guest Editors: Monica Cantile, Francesco Longo, and Franco Fulciniti

Contents

Hindawi Publishing Corporation
BioMed Research International
Volume 2016, Article ID 2850502, 1 page
http://dx.doi.org/10.1155/2016/2850502

Editorial

New Prognostic and Predictive Markers in Head and Neck Tumors

Monica Cantile,[1] Francesco Longo,[2] Gerardo Botti,[1] and Franco Fulciniti[3]

[1]*Pathology Unit, Istituto Nazionale Tumori Fondazione "G. Pascale", IRCCS, 80131 Naples, Italy*
[2]*Head and Neck Surgical Oncology Unit, Istituto Nazionale Tumori Fondazione "G. Pascale", 80131 Naples, Italy*
[3]*Clinical Cytopathology Service, Institute of Pathology, Locarno, Switzerland*

Correspondence should be addressed to Monica Cantile; monica.cantile@libero.it

Received 9 December 2015; Accepted 10 December 2015

Head and neck cancers include a large and heterogeneous group of tumors with a very variable prognosis. These tumors arise from the squamous epithelial lining of the oral cavity, oropharynx, nasopharynx, hypopharynx, and larynx but include also lesions that arise from other anatomical sites, including the salivary glands, the mucosa of respiratory sinuses, thyroid, skin, and orbit. Sometimes, also cerebral tumors are included in this clinic-pathological chapter.

The molecular mechanisms associated with the pathogenesis and evolution of these diseases are poorly understood, although some recent indications, from gene expression profiling studies, suggested a series of well-characterized and new biomarkers able to diagnose and predict behavior and sensitivity to treatment of head and neck cancers.

The expression analysis of these biomarkers associated with histomorphological data could then provide the oncologist with the opportunity to create a proper stratification of patients for customized therapies.

In this special issue the authors contributed to highlighting the appearance and the relative importance of new prognostic markers and of innovative surgical approaches in the prognostic determinism of several head and neck tumors. In particular, T. Ius et al. analyzed factors influencing the tumor recurrence (TR) in a cohort of adult patients with an initial diagnosis of insular Low-Grade Gliomas that underwent a second surgery, without any adjuvant treatments between surgeries, showing that the extent of surgical resection (EOR) at first surgery represents the major predictive factor for TR. Another interesting study by V. Uloza et al. showed the first morphological and morphometric characterization of laryngeal squamous cell carcinoma on an animal model. Regarding the definition of new prognostic biomarkers, M. Tang et al. highlighted that macrophage inflammatory protein-3 alpha (MIP-3α) and cystatin A could represent valuable prognostic markers in nasopharyngeal carcinoma. Moreover, E. Lakiotaki et al. analyzed the clinical significance of cannabinoids CB1 and CB2 in thyroid lesions, underlining especially the usefulness and therapeutic potential of CB2. Finally, M. Hühns et al. showed that HHV-8 and EBV infection are not associated with salivary gland tumors, while HPV infection may play an important role in development and progression of these tumors.

We hope that the information included in this special issue can contribute to understanding of mechanisms associated with the pathogenesis and evolution of head and neck tumors.

Monica Cantile
Francesco Longo
Gerardo Botti
Franco Fulciniti

Hindawi Publishing Corporation
BioMed Research International
Volume 2015, Article ID 617143, 6 pages
http://dx.doi.org/10.1155/2015/617143

Research Article

Expression and Prognostic Significance of Macrophage Inflammatory Protein-3 Alpha and Cystatin A in Nasopharyngeal Carcinoma

Minzhong Tang,[1,2] Ningjiang Ou,[2] Cheng Li,[3] Aiying Lu,[1,2] Jun Li,[1,2] Liping Ma,[3] Weiming Zhong,[4] Jianquan Gao,[4] Yuming Zheng,[1] and Yonglin Cai[1,2]

[1] *Wuzhou Health System Key Laboratory for Nasopharyngeal Carcinoma Etiology and Molecular Mechanism, Wuzhou, Guangxi 543002, China*
[2] *Department of Clinical Laboratory, Wuzhou Red Cross Hospital, Wuzhou, Guangxi 543002, China*
[3] *Department of Pathology, Wuzhou Red Cross Hospital, Wuzhou, Guangxi 543002, China*
[4] *Department of Radiation Oncology, Wuzhou Red Cross Hospital, Wuzhou, Guangxi 543002, China*

Correspondence should be addressed to Yonglin Cai; cylzen@hotmail.com

Received 18 May 2015; Revised 14 October 2015; Accepted 19 October 2015

Academic Editor: Monica Cantile

This study aims to investigate the expression of macrophage inflammatory protein-3 alpha (MIP-3α) and cystatin A in nasopharyngeal carcinoma (NPC) and their association with clinical characteristics and prognosis. Primary tumor specimens from 114 NPC patients and associated clinical follow-up data were collected, and the expression of MIP-3α and cystatin A proteins was investigated by immunohistochemistry. Expression of MIP-3α was significantly associated with TNM stage in patients with NPC ($P < 0.05$). NPC patients with positive expression of MIP-3α exhibited shorter median overall survival (OS) and distant metastasis-free survival (DMFS), compared with patients with negative expression (OS: 50.5 months versus 59.0 months, $P = 0.013$; DMFS: 50.1 months versus 60.2 months, $P = 0.003$). NPC patients with positive expression of cystatin A exhibited shorter median OS, local recurrence-free survival (LRFS), and DMFS, compared with patients with negative expression (OS: 51.1 months versus 60.0 months, $P = 0.004$; LRFS: 54.5 months versus 59.5 months, $P = 0.036$; DMFS: 52.3 months versus 58.8 months, $P = 0.036$). Both MIP-3α and cystatin A overexpressions in NPC tumor tissues were strong independent factors of poor prognosis in NPC patients. MIP-3α and cystatin A expressions may be valuable prognostic markers in NPC patients.

1. Introduction

Recent studies demonstrated that chemokines may play important roles in tumor proliferation and metastasis. Chemokines may be divided into four categories (CC, CXC, CX_3C, and XC), in accordance with the relative positions of conserved cysteine residues [1]. Macrophage inflammatory protein-3 alpha (MIP-3α), encoded by the *CCL20* gene, regulates leukocyte trafficking through lymphoid tissues and induces leukocyte migration into sites of inflammation [2]. Previous reports indicate that MIP-3α expression is increased at certain inflammatory sites and tumors, including hepatocellular carcinoma [3] and pancreatic carcinoma [4]. MIP-3α also interacts with its receptor, CCR6, to promote the growth, migration, and invasion of pancreatic cancer cells.

Impairment of the basement membrane is considered an important marker of cancer invasion, and degradation of the extracellular matrix by proteolytic enzymes is a critical step in cancer cell invasion and metastasis. The proteolytic enzymes of the extracellular matrix, lysosomal cysteine proteases such as cathepsins B and L, as well as their endogenous inhibitors, cystatins, for example, cystatin A (also known as stefin A), cystatin B, and cystatin C, may play important roles in cancer progression and metastasis [5].

To date, radiation therapy is the preferred treatment for nasopharyngeal carcinoma (NPC) without distant metastasis. The local control rate of NPC is close to 100% because of continuing progression in imaging techniques and radiotherapy and the application of concurrent chemoradiotherapy [6,

7]. However, distant metastasis after treatment is a common cause of treatment failure, with a 5-year distant metastasis rate of 20%–32% in NPC patients [8, 9]. Previously, we showed that MIP-3α and cystatin A may be used to predict short-term clinical outcome in patients with NPC [10]. In this study, we evaluated the expression of MIP-3α and cystatin A in NPC tissues and correlated their expression with clinical characteristics and prognosis.

2. Materials and Methods

2.1. Patients. A total of 114 NPC patients, hospitalized in Wuzhou Red Cross Hospital between February 2009 and May 2010, who were previously untreated and biopsy proven and with no evidence of distant metastasis were included prospectively in this study (82 male patients, 32 female patients; median age 48 years, range 26–76 years). Patients were not treated by radiotherapy or chemotherapy prior to the biopsy. Cancer stage was defined according to the Chinese 2008 staging system [11]. All patients underwent radical radiotherapy for NPC. The accumulated doses to gross primary tumor and involved neck lymph nodes were 68–74 Gy and 64–70 Gy, respectively, and the uninvolved areas received 50–56 Gy. Patients with stage I-II NPC were treated by radiotherapy alone, whereas, for patients with stages III-IVa, chemotherapy was added to radiotherapy. This study was approved by the Clinical Research Ethics Committee of Wuzhou Red Cross Hospital.

2.2. Immunohistochemistry. Primary antibodies, including rabbit anti-MIP-3α antibody (ab85032, polyclonal; Abcam, Cambridge, UK), mouse anti-CCR6 (ab93086, monoclonal; Abcam), and mouse anti-cystatin A antibody (ab10442, monoclonal; Abcam), were diluted to 1 : 400, 1 : 500, and 1 : 400, respectively. Briefly, tissue sections were deparaffinized and dehydrated with xylene and ethanol. Antigen retrieval was performed by microwave heating, and sections were then incubated with hydrogen peroxide for 10 min and blocked with normal serum for 10 min, followed by incubation with primary antibody for 1 h. Detection was performed using a streptavidin-HRP kit (Nichirei, Tokyo, Japan) and sections were developed with diaminobenzidine (DAB). Tissues from human liver cancer and thymus tissue were used as positive controls for MIP-3α and cystatin A, respectively. Negative control sections were treated similarly with phosphate-buffered saline (PBS) instead of primary antibody.

The immunostaining results were evaluated and scored independently by two pathologists without knowledge of the clinicopathological outcomes of the patients. MIP-3α, CCR6, and cystatin A staining results were scored as four levels according to the percentage of cytoplasmic and/or membrane positive cells in 10 high-power fields as follows: (−): less than 10%, (+): 11%–20%, (++): 21%–50%, and (+++): >50%. Positive expression of MIP-3α, CCR6, and cystatin A was defined as >10% tumor cells with positive staining, whereas negative expression of MIP-3α, CCR6, and cystatin A was defined as <10% positive staining tumor cells.

2.3. Statistical Analyses. The frequency distribution of categorical variables was tested using a Chi-square test. The overall survival (OS) was calculated from the first day of chemoradiotherapy until the date of death or until the date of the last follow-up (January 26, 2014). The local recurrence-free survival (LRFS) was calculated from the first day of chemoradiotherapy until the date of either primary lesions in the nasopharynx or regional lymph node recurrence or until the date of the last follow-up. Distant metastasis-free survival (DMFS) was calculated from the first day of chemoradiotherapy until the date of distant metastasis or until the date of the last follow-up. Univariate analysis of patient survival was performed using the Kaplan-Meier method and log-rank comparison to evaluate differences between the survival curves. Multivariate analysis was performed using the Cox proportional hazards regression model and a forward stepwise logistic regression approach. There was a statistical difference when the P value was <0.05. Statistical analysis was performed using SPSS software version 13.0 (Chicago, IL, USA).

3. Results

3.1. MIP-3α and Cystatin A Expression in NPC Tissues and Association with Clinicopathological Characteristics. Immunohistochemical analysis of NPC tissues revealed that MIP-3α and cystatin A were predominantly expressed in the cytoplasm of cells in the cancer nests, and CCR6 was expressed in the cell membrane (Figure 1). MIP-3α was positively expressed in 57.9% (66/114) of tumor tissues. CCR6 was positively expressed in 44.7% (51/114) of tumor tissues. There was a significantly positive correlation in the expression of MIP-3α and CCR6 ($r = 0.696$, $P < 0.001$). MIP-3α expression was significantly higher in patients with stage III-IVa tumors compared with those with stage I-II tumors ($P = 0.039$; Table 1). In contrast, MIP-3α expression was not significantly associated with age, sex, pathologic type, tumor (T) classification, or lymph node (N) classification ($P > 0.05$; Table 1).

Cystatin A was positively expressed in 62.3% (71/114) of tumor tissues, and expression was associated with age ($P = 0.009$; Table 1), but not with sex, pathologic type, or stage ($P > 0.05$; Table 1).

3.2. Univariate Survival Analysis. After a median follow-up of 53 months (range 5–61 months), the median OS, LRFS, and DMFS for all patients were 54.5 months, 56.6 months, and 54.9 months, respectively. The OS, LRFS, and DMFS curves for the positive and negative MIP-3α expression groups are shown in Figure 2. The median OS and DMFS were significantly poorer in patients with positive MIP-3α expression compared with patients with negative MIP-3α expression (OS: 50.5 months versus 59.0 months, $P = 0.013$, Figure 2(a); DMFS: 50.1 months versus 60.2 months, $P = 0.003$, Figure 2(c)). There was no statistical difference in median LRFS between the two groups (54.2 months versus 58.7 months, $P = 0.503$, Figure 2(b)).

The OS, LRFS, and DMFS curves for the positive and negative cystatin A expression groups are shown in Figure 2.

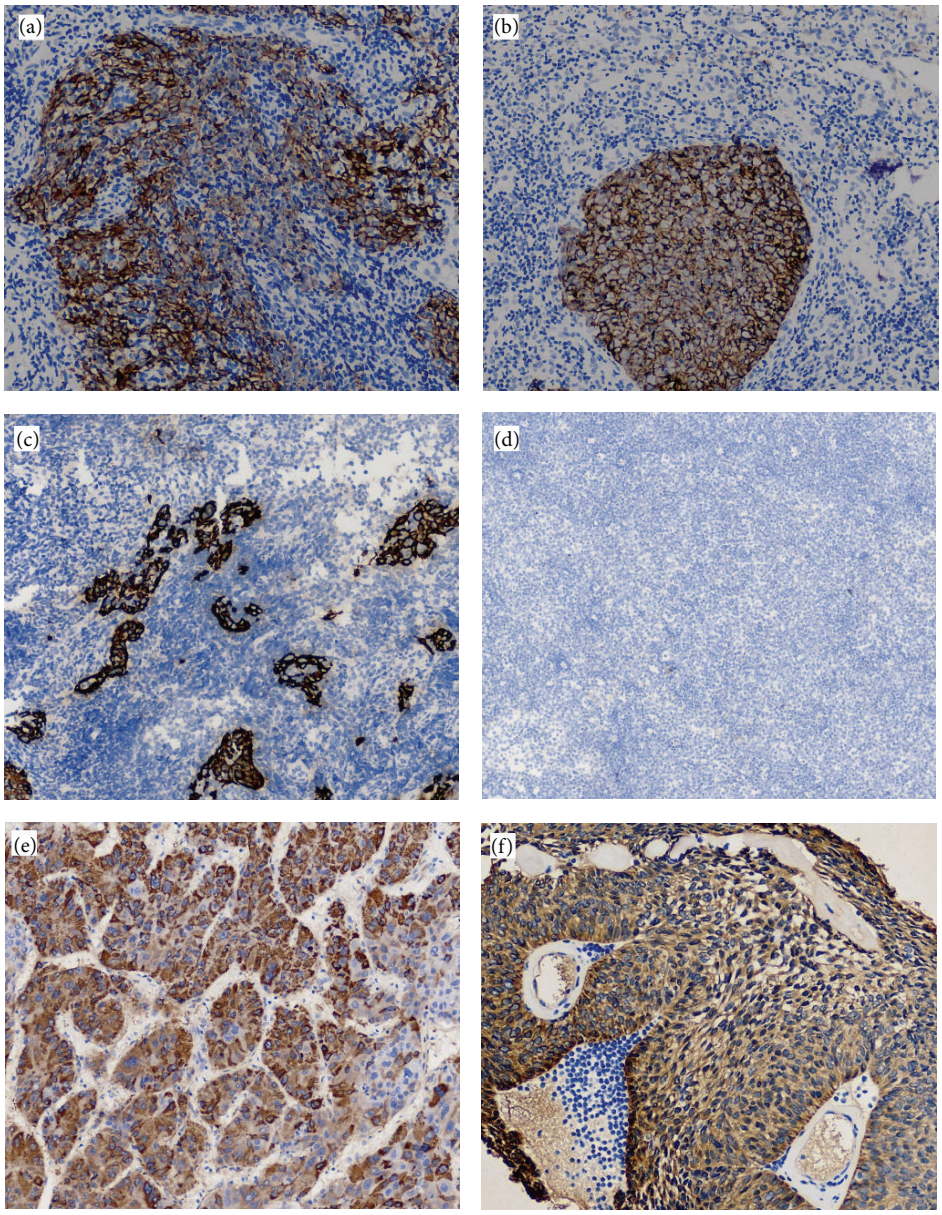

Figure 1: Immunohistochemistry staining of nasopharyngeal carcinoma (NPC) tissues (original magnification, ×200). (a) Positive expression of MIP-3α in NPC tissue. (b) Positive expression of cystatin A in NPC tissue. (c) Positive expression of CCR6 in NPC tissue. (d) Negative expression in NPC tissue as negative control. (e) Positive expression of MIP-3α in liver cancer tissue as positive control. (f) Positive expression of cystatin A in thymus tissue as positive control.

The median OS, LRFS, and DMFS were significantly poorer in patients with positive cystatin A expression compared with patients with negative cystatin A expression (OS: 51.1 months versus 60.0 months, $P = 0.004$, Figure 2(d); LRFS: 54.5 months versus 59.5 months, $P = 0.036$, Figure 2(e); DMFS: 52.3 months versus 58.8 months, $P = 0.036$, Figure 2(f)).

3.3. Multivariate Analysis. The association of MIP-3α and cystatin A expression with OS, LRFS, and DMFS was examined further with Cox proportional hazards regression modeling, with adjustment for age, gender, WHO pathological classification, T classification, N classification, and chemotherapy. These analyses revealed that positive cystatin A expression, T classification, and N classification were independent prognostic factors of OS in NPC patients; T classification was an independent prognostic factor of LRFS; and age $\geq$ 45 years, N classification, and positive MIP-3α expression were also independent prognostic factors of DMFS (Table 2).

4. Discussion

Chemokines, which can direct cellular chemotactic movement, are low molecular weight cytokines secreted by various cell types. Most tumor cells express a wide range of chemokines and chemokine receptors and are in turn

Table 1: Correlation of expression of MIP-3α and cystatin A with clinical characteristics in 114 NPC patients [n (%)].

Characteristics	Number of patients	MIP-3α			Cystatin A		
		Negative	Positive	P value	Negative	Positive	P value
Age				0.197			0.009
<45 years	41	14	27		22	19	
≥45 years	73	34	39		21	52	
Gender				0.286			0.208
Male	82	32	50		28	54	
Female	32	16	16		15	17	
Pathology (WHO)*							
Type I	1	0	1	0.952	0	1	0.722
Type II	12	5	7		4	8	
Type III	101	43	58		39	62	
T classification				0.145			0.100
T1-2	55	27	28		25	30	
T3-4	59	21	38		18	41	
N classification				0.117			0.861
N0-1	36	19	17		14	22	
N2-3	78	29	49		29	49	
Overall stage				0.039			0.181
I-II	15	10	5		8	7	
III-IVa	99	38	61		35	64	

*Type I: keratinizing squamous cell carcinoma; type II: differentiated nonkeratinizing carcinoma; type III: undifferentiated nonkeratinizing carcinoma (according to World Health Organization histological classification).

Table 2: Multivariate analysis of prognostic factors using Cox proportional hazard ratio model.

Endpoint	Hazard ratio (95% CI)	P value
Overall survival		
T classification: T3-4 versus T1-2	4.66 (1.50–14.52)	0.008
N classification: N3 versus N0-2	4.16 (1.39–12.45)	0.011
Cystatin A: (+) versus (−)	4.93 (1.12–21.63)	0.035
Local recurrence-free survival		
T classification: T3-4 versus T1-2	12.99 (1.69–100.02)	0.014
Distant metastasis-free survival		
Age: ≥45 y versus <45 y	3.57 (1.07–11.89)	0.038
N classification: N3 versus N0-2	3.66 (1.12–12.02)	0.032
MIP-3α: (+) versus (−)	8.10 (1.82–35.93)	0.006

CI = confidence interval.

regulated by a complex network of chemokines and their associated receptors. Increased expression of MIP-3α has been reported in multiple myeloma [12], hepatocellular carcinoma [13], and oral cavity squamous cell carcinoma [14]. MIP-3α, through its CCR6 receptor, promotes tumor cell invasion in pancreatic adenocarcinoma [4]. In this study, we demonstrate that MIP-3α is positively expressed in 57.9% of NPC tissues. This suggests that NPC, like other cancers, exhibits high expression of MIP-3α. By analyzing the relationship between MIP-3α expression and clinical characteristics and prognostic factors, we found that patients with advanced stage NPC were more likely to have higher MIP-3α expression. Positive MIP-3α expression in patients with NPC was significantly associated with poorer OS and DMFS. MIP-3α is a powerful chemoattractant for T cells and immature dendritic cells, and regulatory T cells are recruited to NPC lesions to enhance local immunosuppression and help NPC cells evade antitumor immune responses. MIP-3α also appears to promote tumor cell proliferation and metastasis by attracting endothelial cells, accelerating angiogenesis, and affecting cancer cell mobility.

The ability to invade surrounding tissues and metastasize is an important feature of cancers. Penetration and degradation of components of the extracellular matrix and basement membrane are key steps in the metastatic process of cancer cells. The expression of specific proteolytic enzymes is triggered, and these enzymes are subsequently secreted and activated during the metastatic process. Proteolytic enzymes including serine proteases, matrix metalloproteinases, and lysosomal cysteine proteinase cathepsin B are strongly correlated with the metastatic state of cancer cells. The interaction between cathepsins and cystatins contributes to the degradation and remodeling of the extracellular matrix during cancer cell growth, angiogenesis, invasion, and metastasis [5]. Higher levels of cystatin A in body fluids have been associated with a poor prognosis in cancer patients [15]. In this study, positive cystatin A expression in patients with NPC was significantly associated with poorer OS, LRFS, and DMFS compared with those patients with negative cystatin A expression.

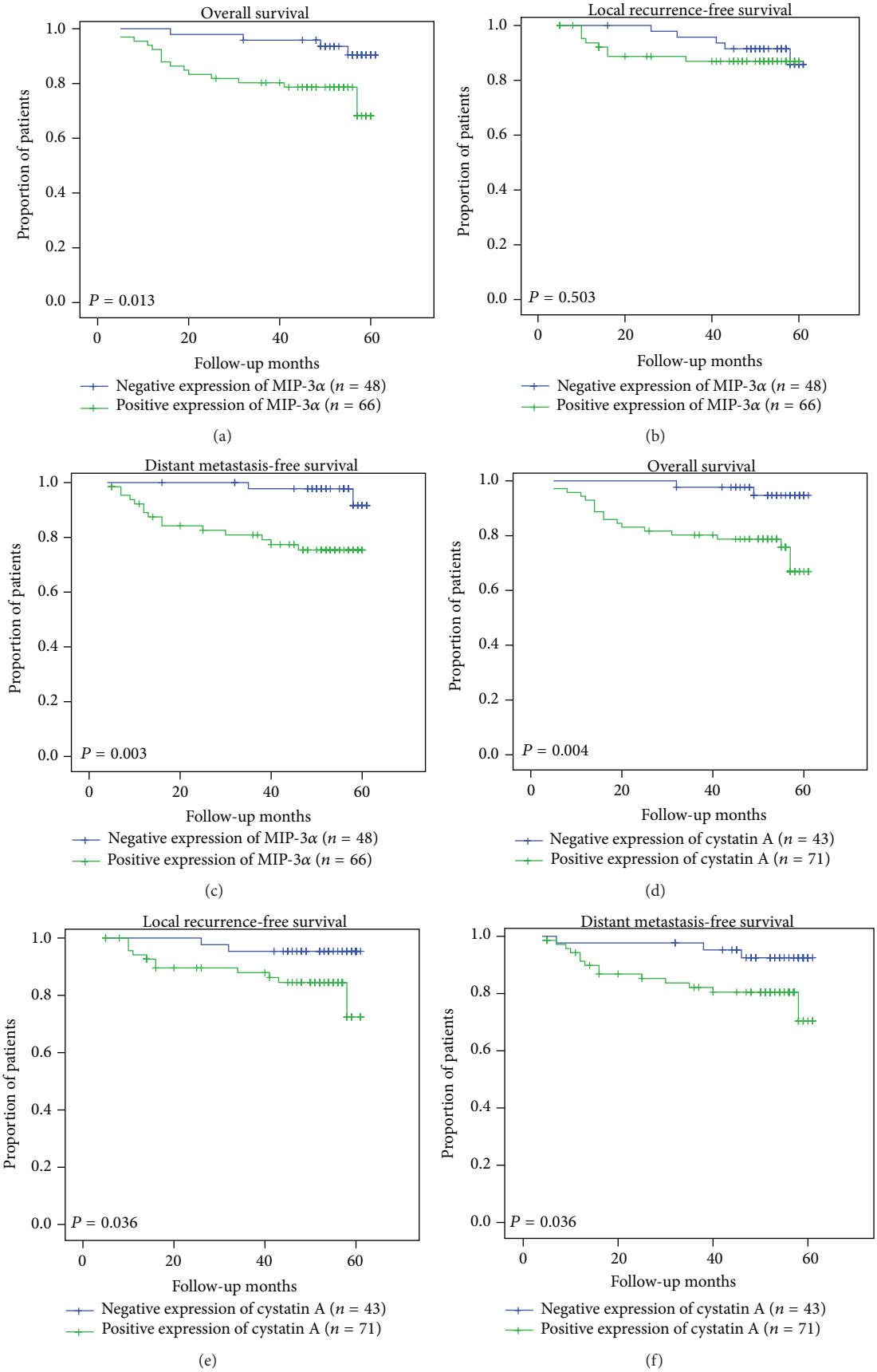

Figure 2: Kaplan-Meier curves of 114 NPC patients. Overall survival (a), local recurrence-free survival (b), and distant metastasis-free survival (c) of 114 NPC patients, stratified according to MIP-3α expression. Overall survival (d), local recurrence-free survival (e), and distant metastasis-free survival (f) of 114 NPC patients stratified according to cystatin A expression.

In multivariate analysis, we statistically weighted MIP-3α and cystatin A with clinicopathological characteristics to assess their relative prognostic impact. The tumor (T) classification and lymph node (N) classification remained powerful predictors of survival for NPC patients. MIP-3α and cystatin A were also independent prognostic factors.

5. Conclusion

Our results indicate that MIP-3α and cystatin A exhibit significant prognostic value in patients with NPC. Patients with positive expression of MIP-3α or cystatin A exhibited a poorer prognosis than those with negative expression of MIP-3α and cystatin A. On the basis of the presented results, additional studies are required (a) to evaluate the prognostic relevance of both factors in a more homogeneous and larger cohort of NPC patients; (b) to determine the value of their clinical applicability with respect to the selection of treatment in individual patients with this type of cancer; and (c) to investigate the mechanism of the two factors in the distant metastasis of NPC.

Conflict of Interests

The authors declare that there is no conflict of interests.

Authors' Contribution

Minzhong Tang and Ningjiang Ou contributed equally to this study.

Acknowledgments

This study was funded by the Science and Technology Project Foundations of Guangxi, China (no. 11194011), and the Hi-Tech Research and Development Program of China (no. 2012AA02A501).

References

[1] I. F. Charo and R. M. Ransohoff, "The many roles of chemokines and chemokine receptors in inflammation," *The New England Journal of Medicine*, vol. 354, no. 6, pp. 610–621, 2006.

[2] G. Lazennec and A. Richmond, "Chemokines and chemokine receptors: new insights into cancer-related inflammation," *Trends in Molecular Medicine*, vol. 16, no. 3, pp. 133–144, 2010.

[3] Y.-T. Shih, M.-C. Wang, H.-H. Peng et al., "Modulation of chemotactic and pro-inflammatory activities of endothelial progenitor cells by hepatocellular carcinoma," *Cellular Signalling*, vol. 24, no. 3, pp. 779–793, 2012.

[4] A. S. Campbell, D. Albo, T. F. Kimsey, S. L. White, and T. N. Wang, "Macrophage inflammatory protein-3α promotes pancreatic cancer cell invasion," *Journal of Surgical Research*, vol. 123, no. 1, pp. 96–101, 2005.

[5] Š. Magister and J. Kos, "Cystatins in immune system," *Journal of Cancer*, vol. 4, no. 1, pp. 45–56, 2013.

[6] L. Chen, C.-S. Hu, X.-Z. Chen et al., "Concurrent chemoradiotherapy plus adjuvant chemotherapy versus concurrent chemoradiotherapy alone in patients with locoregionally advanced nasopharyngeal carcinoma: a phase 3 multicentre randomised controlled trial," *The Lancet Oncology*, vol. 13, no. 2, pp. 163–171, 2012.

[7] T. Dechaphunkul, K. Pruegsanusak, D. Sangthawan, and P. Sunpaweravong, "Concurrent chemoradiotherapy with carboplatin followed by carboplatin and 5-fluorouracil in locally advanced nasopharyngeal carcinoma," *Head and Neck Oncology*, vol. 3, article 30, 2011.

[8] T. Xu, C. Hu, X. Wang, and C. Shen, "Role of chemoradiotherapy in intermediate prognosis nasopharyngeal carcinoma," *Oral Oncology*, vol. 47, no. 5, pp. 408–413, 2011.

[9] A. W. M. Lee, S. Y. Tung, R. K. C. Ngan et al., "Factors contributing to the efficacy of concurrent-adjuvant chemotherapy for locoregionally advanced nasopharyngeal carcinoma: combined analyses of NPC-9901 and NPC-9902 Trials," *European Journal of Cancer*, vol. 47, no. 5, pp. 656–666, 2011.

[10] J. Li, M. Z. Tang, A. Y. Lu et al., "Expression of serum MIP-3α and cystatin A in patients with nasopharyngeal carcinoma and their clinical significance," *China Oncology*, vol. 23, no. 10, pp. 845–851, 2013.

[11] Committee of Chinese Clinical Staging of Nasopharyngeal Carcinoma, "Report on the revision of nasopharyngeal carcinoma '92 staging," *Chinese Journal of Radiation Oncology*, vol. 18, no. 1, pp. 2–6, 2009.

[12] N. Giuliani, G. Lisignoli, S. Colla et al., "CC-Chemokine ligand 20/macrophage inflammatory protein-3α and CC-chemokine receptor 6 are overexpressed in myeloma microenvironment related to osteolytic bone lesions," *Cancer Research*, vol. 68, no. 16, pp. 6840–6850, 2008.

[13] K. Yamauchi, S. M. F. Akbar, N. Horiike, K. Michitaka, and M. Onji, "Increased serum levels of macrophage inflammatory protein-3alpha in hepatocellular carcinoma: relationship with clinical factors and prognostic importance during therapy," *International Journal of Molecular Medicine*, vol. 11, no. 5, pp. 601–605, 2003.

[14] K.-P. Chang, H.-K. Kao, T.-C. Yen et al., "Overexpression of macrophage inflammatory protein-3alpha in oral cavity squamous cell carcinoma is associated with nodal metastasis," *Oral Oncology*, vol. 47, no. 2, pp. 108–113, 2011.

[15] J. Kos, B. Werle, T. Lah, and N. Brunner, "Cysteine proteinases and their inhibitors in extracellular fluids: markers for diagnosis and prognosis in cancer," *International Journal of Biological Markers*, vol. 15, no. 1, pp. 84–89, 2000.

Hindawi Publishing Corporation
BioMed Research International
Volume 2015, Article ID 829349, 7 pages
http://dx.doi.org/10.1155/2015/829349

Research Article

HPV Infection, but Not EBV or HHV-8 Infection, Is Associated with Salivary Gland Tumours

Maja Hühns,[1] Georg Simm,[1] Andreas Erbersdobler,[1] and Annette Zimpfer[1,2]

[1]*Institute of Pathology, University of Rostock, Strempelstrasse 14, 18055 Rostock, Germany*
[2]*Institute of Pathology, University Medical Centre Jena, Ziegelmühlenweg 1, 07743 Jena, Germany*

Correspondence should be addressed to Maja Hühns; maja.huehns@med.uni-rostock.de

Received 1 July 2015; Accepted 21 October 2015

Academic Editor: Monica Cantile

Benign and malignant salivary gland tumours are clinically heterogeneous and show different histology. Little is known about the role of human herpes virus 8 (HHV-8), Epstein-Barr virus (EBV), and human papillomavirus (HPV) infection in salivary gland neoplasms. We investigated the presence of the three viruses in formalin-fixed, paraffin-embedded tissue samples in a cohort of 200 different salivary gland tumours. We performed EBV-LMP-1 and HHV-8 and p16 immunohistochemistry, a specific chip based hybridization assay for detection and typing of HPV and a chromogenic in situ hybridization for EBV analysis. Only one case, a polymorphic low-grade carcinoma, showed HHV-8 expression and one lymphoepithelial carcinoma was infected by EBV. In 17 cases (9%) moderate or strong nuclear and cytoplasmic p16 expression was detected. The HPV type was investigated in all of these cases and additionally in 8 Warthin's tumours. In 19 cases HPV type 16 was detected, mostly in Warthin's tumour, adenoid cystic carcinoma, and adenocarcinoma NOS. We concluded that HHV-8 infection and EBV infection are not associated with salivary gland cancer, but HPV infection may play a role in these tumour entities.

1. Introduction

Benign and malignant salivary gland tumours belong to rare head and neck tumours. Most cases are benign and only 20% are malignant [1]. The majority of the diseases arise in the sixth decade and the sex distribution is equal [2]. Salivary gland tumours show a wide range of phenotypic, biological, and clinical heterogeneity [3]. They occur in the major and minor salivary glands, whereof 80% of major salivary gland tumours are present in the parotid glands, and less than half of these tumours are malignant [3].

In general, several viruses have been demonstrated to be the trigger of neoplastic diseases of the head and neck, like human papillomavirus (HPV) [4] and different human herpes viruses, like human herpes virus-4/Epstein-Barr virus (EBV) [5], cytomegalovirus (CMV) [6], and human herpes virus 8 (HHV-8) [7]. However, the role of viruses in the genesis of salivary gland tumours remains still debatable.

The aim of the present study was to determine the prevalence of different pathogens like HHV-8, EBV, and HPV in a large cohort of salivary gland tumours. The involvement of these three pathogens was analyzed by immunohistochemistry, a specific chip based hybridization assay, or chromogenic in situ hybridization.

2. Material and Methods

2.1. Patients. A total of 200 patients with salivary gland tumours were included, diagnosed between 1990 and 2014 (Table 1). Among those there were 93 malignant and 107 benign tumours of different entities (Table 2). The formalin-fixed, paraffin embedded specimens were retrieved from the archive of the Institute of Pathology at the University Medicine of Rostock.

The study was performed with internal review board approval and patients' data were anonymized in accordance with German laws concerning safety data.

2.2. Clinical Data. Clinical data were obtained by reviewing the charts of the Clinical Cancer Registry, University of Rostock. These data were anonymized and included sex, age at diagnosis, and stage (Tables 1 and 2).

Table 1: Patient characteristics of salivary gland tumours.

Clinical characteristics	$n = 200$
Median age, years	59.9
Range	11–95
Sex	
Male	107 (53.5%)
Female	93 (46.5%)
Tumour location	
Parotid gland	175 (87.5%)
Left side	84 (48%)
Right side	69 (39.5%)
Submandibular gland	14 (7%)
Left side	7 (3.5%)
Right side	7 (3.5%)
Minor salivary glands	11 (5.5%)
Stage at presentation (malignant)	
I	36 (38.7%)
II	18 (19.4%)
III	20 (21.5%)
IV	17 (18.3%)
No stadium determinable	2 (2.2%)

2.3. Construction of Tissue Microarrays (TMA). For TMA construction, a hematoxylin and eosin (H&E) stained slide from each block was used to define the representative tumour and normal region by an experienced pathologist. Tissue cylinders with a diameter of 1.0 mm were punched from the specimen block and brought into an empty paraffin block [8] by using a precision instrument (Beecher Instruments, Silver Spring, MD, USA). Three tissue cylinders of tumour and one cylinder with normal tissue from every specimen were prepared. Taken together, 10 different TMA blocks with malignant and benign specimens were constructed.

2.4. Immunohistochemistry. For each TMA block, four-micrometer sections were transferred to an adhesive-coated glass slide system (Instrumedics Inc, Hackensack, NJ, USA) and stained with H&E. Only cases containing at least 10% tumour tissue were further analyzed.

Immunohistochemical staining was performed with an autostainer (EnVision FLEX, High pH, (Link), DAKO, Hamburg, Germany) according to the manufacturer's standard protocol with primary antibodies against Cytokeratin AE1/AE3 (monoclonal mouse, reference number: C1702C01, titre 1 : 500, DCS, Hamburg, Germany), EBV-latent membrane protein-1 (LMP-1) (monoclonal mouse, clones CS.1–4, "ready to use," Dako, Hamburg, Germany), HHV-8 (monoclonal mouse, 1 : 50, reference number 6011336, Leica, Wetzlar, Germany), and p16 (monoclonal mouse, clone G175-405, 1 : 20, BD Biosciences, Heidelberg, Germany).

Cytokeratin AE1/AE3 immunohistochemistry served as a positive control for the tissue studied and proved the stainability of the archival material.

For LMP1 of EBV the presence of unequivocal membranous and cytoplasmatic staining in >2% of tumour cells was considered positive. For HHV-8 the presence of nuclear immunoreactivity in >2% of tumour cells was considered positive. Positivity for p16 was considered when a moderate to strong staining was observed in the cytoplasm and in the nucleus. The staining intensities were graded as negative, weak, moderate, and strong by visual inspection by an experienced pathologist. Weak and patchy p16 signalling was judged as negative. For positive controls, (tumour) tissues with known marker expression were carried along. The positive controls were as follows: HHV8: Kaposi sarcoma in an AIDS patient; EBV-LMP-1: tonsil with a known infectious mononucleosis (EBV positive); EBER-CISH: tonsil with a known infectious mononucleosis (EBV positive); P16: carcinoma of the tonsil with a known HPV infection.

In the negative control experiments, the primary antibodies were omitted.

2.5. Detection of EBV. Chromogenic in situ hybridization (CISH) staining for EBV encoded RNA (EBER) transcripts was performed on 4 μm deparaffinized tissue sections, mounted on adhesive coated glass slides according to manufacturer's instructions (ZytoVision, Bremerhaven, Germany). Slides were digested with pepsin solution for 10 minutes, incubated with biotin-labelled ZytoFast EBV probe for 60 minutes at 55°C, followed by incubation with AP-streptavidin for 30 minutes at 37°C, and colouring was performed with NBT/BZIP at 37°C for maximal 40 minutes. Cells exhibiting nuclear staining were considered positive. Positive and negative controls were included in each run.

2.6. Identification of HPV Types. The cases selected for molecular HPV analysis were all tumours with moderate or strong cytoplasmic and nuclear p16 expression and additionally in 8 Warthin's tumours. Tumour DNA was extracted from formalin-fixed, paraffin embedded sections in 25 salivary gland cancers with the ReliaPrep FFPE gDNA Miniprep system (Promega, Mannheim, Germany) according to manufacturers' instruction. For identification of HPV types the HPV Type 3.5 LCD-Array Kit (Chipron, Berlin, Germany) was used according to manufacturer's instructions. Briefly, two PCR reactions were performed using supplied My11/09 (product size 450 bp) and "125" (product size 125 bp) primer mixes and analyzed by agarose gel electrophoresis. Both PCR products were mixed and hybridized on the 3.5 LCD chip slide. The slide was subsequently scanned on the Slide Reader Scanner and evaluated with the Slide Reader Software (Chipron, Berlin, Germany).

3. Results

3.1. Patient and Tumour Characteristics. We analyzed 200 patients with malignant or benign salivary gland tumours, diagnosed between 1990 and 2014 (Table 1). The mean age at diagnosis was 58.9 years (range 11–95 years), 107 were male (53.5%), and 93 were female (46.5%). Different tumour entities were included, whereas in malignant tumours mainly mucoepidermoid carcinoma (18.3%), adenoid cystic carcinoma (17.2%), and adenocarcinoma NOS (10.8%) occurred.

Table 2: Tumour characteristics of malignant and benign tumours ($n = 200$).

	Type of tumour	Number of cases	Frequency in %
Malignant	Mucoepidermoid carcinoma	17	18.3
	Adenoid cystic carcinoma	16	17.2
	Adenocarcinoma NOS	10	10.8
	Salivary duct carcinoma	9	9.7
	Acinus cell carcinoma	7	7.5
	Adenoid basal-cell carcinoma	5	5.4
	Squamous cell carcinoma	5	5.4
	Nonkeratinized squamous cell carcinoma	4	4.3
	Keratinized squamous cell carcinoma	4	4.3
	Oncocytic carcinoma	2	2.2
	Lymphoepithelial carcinoma	2	2.2
	Micropapillary carcinoma	2	2.2
	Myoepithelial carcinoma	5	5.4
	Pseudo sarcomatoid carcinoma	1	1.1
	Polymorphic low-grade carcinoma	1	1.1
	Undifferentiated carcinoma	1	1.1
	Cystadenocarcinoma	1	1.1
	Malignant melanoma	1	1.1
Benign	Cystadenolymphoma (Warthin's tumour)	46	43
	Pleomorphic adenoma	33	30.8
	Basal-cell adenoma	15	14.0
	Oncocytoma	7	6.5
	Myoepithelioma	3	2.9
	Cystadenoma	2	1.9
	Adenolyphoma	1	0.9

NOS, not otherwise specified.

In benign tumours basically Warthin's tumours (43%) and pleomorphic adenoma (33%) were diagnosed.

3.2. Morphological Evaluation of the Specimens. 190/200 (95%) of the specimens contained >10% tumour tissue. Ten cases (5%) had limited tumour tissue and were excluded from the study.

3.3. Expression and Detection of HHV-8, EBV, and HPV by Immunohistochemistry. AE1/AE3 positivity was found in 183/190 (96.3%) cases, indicating that most tumours were of epithelial origin and were suitable for further investigations (Figure 1(a)).

Only one case, a polymorphic low-grade carcinoma exhibited HHV-8 expression, located in the nucleus (Figure 1(b)).

A small subfraction of only 4 cases expressed the EBV-LPM-1 protein and just one case, a lymphoepithelial carcinoma, was positive in EBER-CISH analyses (Figures 1(c) and 1(e)).

Moderate or strong nuclear and cytoplasmic p16 was seen in 17/190 (9%) cases (Figure 1(d)). The most frequent tumour type with positive nuclear expression was adenoid cystic carcinoma, followed by adenocarcinoma and acinus cell carcinoma.

3.4. Detection of HPV. Detection of HPV types was performed in all 17 p16 nuclear positive cases and also in 8 Warthin's tumours. In 19/25 cases (76%) HPV type was classified (Table 3); 6 cases were negative or DNA was not amplifiable. In all 19 positive cases HPV type 16 was detected (Figure 1(f)) in different tumour entities (Table 4), mostly in malignant cancer types (12/25) compared to benign tumours (7/25).

4. Discussion

The participation of viruses in salivary gland tumours is receiving increasing interest. The role of EBV in lymphoepithelial carcinomas (LEC), nasopharyngeal carcinomas, and also benign Warthin's tumours was reported in several studies [9, 10]. In our study, we investigated different salivary gland tumours, including 46 Warthin's tumours and two cases of LEC. But EBV was detected only in one LEC (Figures 1(c) and 1(e)). LEC is a rare malignancy and only few cases with EBV infection were described in the literature. It occurs mainly in East Asia population and only rarely in western countries (reviewed in [11]). However, there are many controversies about the association of EBV infection with LEC. Some studies described negative results [12–17], while other authors found a positive association [11, 18–20]. On the basis of our data of only two cases, we are not able

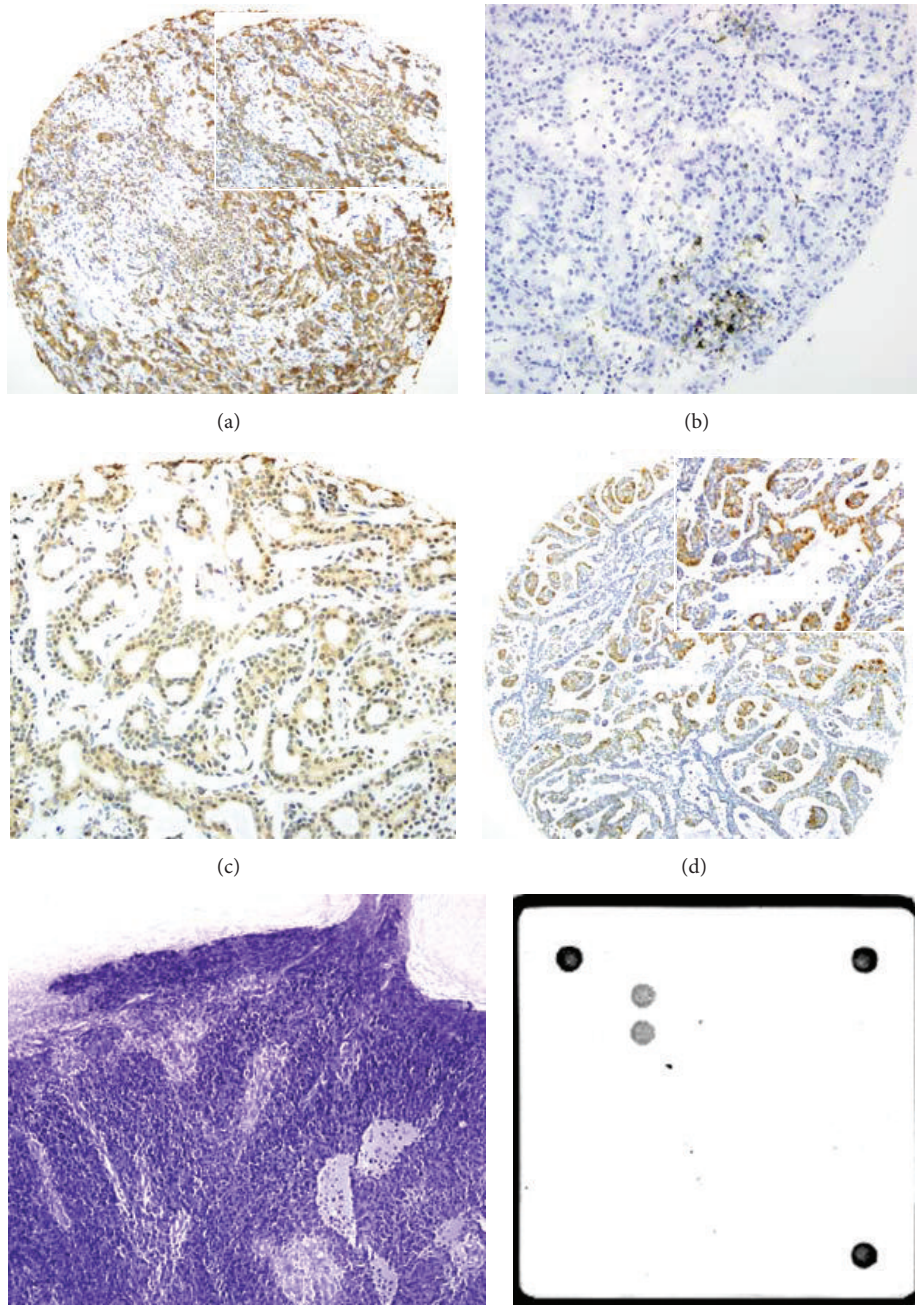

Figure 1: Evidence of pathogens in different salivary gland tumours. (a–d) Immunohistochemistry of (a) AE1/AE3 (10x magnification, in insert 20x magnification) in an adenocarcinoma NOS; (b) HHV-8 (20x magnification) in a polymorphic low-grade carcinoma; (c) EBV-LMP-1 (20x magnification) in a lymphoepithelial carcinoma; and (d) p16 expression (10x magnification, in insert 20x magnification) in an adenoid cystic carcinoma. (e) Lymphoepithelial carcinoma showing EBER expression (10x magnification). (f) Adenoid cystic carcinoma with HPV type 16 detected by Chipron LCD array.

to conclude whether EBV is associated with LEC or not. The presence of EBV in Warthin's tumour was described in several studies, with a ratio of about 20% [9, 21, 22]. However in our study no tumour of this entity showed any positivity for EBV. The present results indicate that infection with EBV does not play a major role in salivary gland neoplasm.

HHV-8, which naturally infects only humans, is known to be involved in various malignancies including Kaposi's sarcoma, Castleman's disease, and primary effusion lymphoma [23–26]. Nevertheless, the role in salivary gland tumours is still unclear. Klussmann et al. reported that HHV-8 has no major tropism to salivary gland epithelium in immunocompetent patients [27]. However, they detected HHV-8 in

Table 3: Expression and detection of HPV, EBV, and HHV-8 in salivary gland tumours by immunohistochemistry, CISH, and chip technology.

	n	Positive	Distribution of malignant cases	Distribution of benign cases	Negative	Not evaluable
HHV-8	190	1 (0.5%)	1	0	187 (98.4%)	2 (1.1%)
EBV-LMP-1	190	4 (2.1%)	3	1	183 (96.3%)	3 (1.6%)
EBER-CISH	190	1 (0.5%)	1	0	187 (98.4%)	2 (1.1%)
p16	190	17 (9%)	14	3	159 (83.5%)	14 (7.5%)
HPV (chip)	25*	19 (76%)	12	7	1 (4%)	5 (20%)

*Cases with strong nuclear p16 positivity and Warthin's tumours; HHV-8, human herpes virus 8; EBV-LMP-1, Epstein-Barr virus latent membrane protein-1; EBER-CISH, Epstein-Barr virus encoded RNA-chromogenic in situ hybridization; p16, cyclin-dependent kinase inhibitor 2A; HPV, human papillomavirus.

Table 4: Distribution of HPV type 16 positive cases in salivary gland tumours ($n = 19$).

	Positive
Adenoid cystic carcinoma	4
Adenocarcinoma NOS	3
Invasive ductal carcinoma	1
Acinus cell carcinoma	2
Adenoid basal-cell carcinoma	2
Warthin's tumour	6
Pleomorphic adenocarcinoma	1

a bilateral MALT-lymphoma of the parotid gland of a HHV-8 seropositive female patient suffering from Sjögren's syndrome [27]. Other reports found out that HHV-8 is uncommon in the saliva of healthy persons but was found in patients with Kaposi's sarcoma [28, 29]. Klussmann et al. concluded that a latent infection of the salivary gland in people from areas with low prevalence of Kaposi's sarcoma is rare [27]. In contrast, in a Greek study HHV-8 was detected in 44% of Warthin's tumour [7]. Our findings differ from the Greek study, since we detected no HHV-8 in our 46 investigated Warthin's tumours. Only in one adenocarcinoma NOS the virus was found.

p16 is a cyclin-dependent kinase inhibitor of CDK4 and CDK6, which activates the negative cell cycle regulator retinoblastoma protein (pRB). This protein in turn downregulates p16 expression. The human papillomavirus oncogene E7 interferes with pRB and inactivates the protein, resulting in overexpression of p16 [30]. Our results showed in 17/190 cases (9%) a nuclear expression of the surrogate marker p16. Nevertheless, p16 is not a specific marker for the detection of HPV [31] and its value in the detection of HPV infection is still controversial [32]. Due to the role of p16 in cell cycle, we selected only the cases with strong nuclear p16 expression for further HPV typing by DNA analysis. Based on all investigated cases, 19 cases were HPV positive (10%). In several studies, a correlation of HPV infection, mainly types 16 and 18, with salivary gland tumours was shown. In American patients with mucoepidermoid carcinoma 36% were positive, predominantly type 16 and less commonly HPV type 18 or types 16 and 18 together [33]. In two other studies similar results were shown for salivary gland tumours. Hafed et al. detected positivity for HPV type 16 and/or type 18 in 23.5% [34], whereas Lin et al. found 35.8% positive HPV cases [9]. In contrast, in other studies with Warthin's tumours no HPV-positive case could be found [32, 35]. In our cohort of salivary gland carcinomas we identified 6 Warthin's tumours infected with HPV type 16, after preselection by p16 expression, according to 13.3% of all investigated Warthin's tumours.

Most positive HPV cases in our study derived from malignant salivary tumours like adenoid cystic carcinoma and adenocarcinoma NOS and, to a lower proportion from acinus cell carcinoma, salivary duct carcinoma and adenoid basal-cell carcinoma. Recent studies also showed conflicting results with malignant tumours. In some studies with up to or more than 100 salivary gland neoplasms, no HPV positive cases were identified [32, 35–37]. In contrast, other studies showed a presence of HPV in these tumour entities [9, 33, 34].

Besides smoking and alcohol consumption, HPV represents another risk factor for squamous head and neck tumours [38]. High-risk (hr) HPV types, often type 16, were frequently detected in oropharynx carcinoma, mainly in tonsillar carcinoma and tongue base carcinoma [38, 39]. Recent advances in HPV-induced cervical precancerous lesions highlight that different pathways of HPV infection (i.e., viral persistent, transient or latent infection, productive or permissive infection) may or may not progress to a "transforming infection," with risk of developing high grade squamous intraepithelial lesion and consecutive invasive cancer [40]. The data show that only a minority of hr HPV infections become "transforming infections," characterised by altered gene expression, especially 2 viral genes E6 and E7 (as discussed above) [40]. Among hr HPV types, type 16 is obviously associated with the greatest risk to develop cervical cancer if left untreated [40, 41]. But which factors determine malignant progression is still poorly understood [40]. And for hr HPV positive head and neck tumours, especially oropharyngeal cancers, data concerning the development and progression of "transforming" hr HPV infections are still limited [26].

Risk factors, like several sexual partners and oral practices, were similar to those of HPV-associated cervix carcinoma [42, 43]. In a recent study, the age for oral HPV infection was dated between 14 and 69 years [44] and is consistent with our results of HPV positive cases (between 31 and 72 years). Due to the growing rates of salivary gland tumours and positivity of HPV types 16 and 18, some studies hypothesized that use of the two available HPV vaccines for cervix carcinoma may cause a reduction of salivary gland cancer [42, 44–46].

5. Conclusion

Salivary gland neoplasm is an uncommon and heterogeneous disease. These tumours are not generally associated with EBV or HHV-8 infection. In our investigations we found a correlation between p16 nuclear overexpression and high-risk HPV infection in salivary gland neoplasm. HPV type 16 was identified in adenoid cystic carcinoma, adenocarcinoma NOS, and Warthin's tumours and, to a lesser extent, in acinus cell carcinoma, salivary duct carcinoma, and adenoid basal-cell carcinoma. HPV seems to be involved in a significant proportion of salivary gland tumours but its exact role is still controversial due to the recent studies.

Conflict of Interests

The authors declare that there is no conflict of interests regarding the publication of this paper.

References

[1] V. S. To, J. Y. Chan, R. K. Tsang, and W. I. Wei, "Review of salivary gland neoplasms," *ISRN Otolaryngology*, vol. 2012, Article ID 872982, 6 pages, 2012.

[2] L. Licitra, C. Grandi, F. J. Prott, J. H. Schornagel, P. Bruzzi, and R. Molinari, "Major and minor salivary glands tumours," *Critical Reviews in Oncology/Hematology*, vol. 45, no. 2, pp. 215–225, 2003.

[3] D. J. Adelstein, S. A. Koyfman, A. K. El-Naggar, and E. Y. Hanna, "Biology and management of salivary gland cancers," *Seminars in Radiation Oncology*, vol. 22, no. 3, pp. 245–253, 2012.

[4] J. M. Boland, E. D. McPhail, J. J. García, J. E. Lewis, and D. J. Schembri-Wismayer, "Detection of human papilloma virus and p16 expression in high-grade adenoid cystic carcinoma of the head and neck," *Modern Pathology*, vol. 25, no. 4, pp. 529–536, 2012.

[5] A. M. Pollock, M. Toner, M. Mcmenamin, J. Walker, and C. I. Timon, "Absence of Epstein-Barr virus encoded RNA and latent membrane protein (LMP1) in salivary gland neoplasms," *Journal of Laryngology and Otology*, vol. 113, no. 10, pp. 906–908, 1999.

[6] M. Melnick, P. P. Sedghizadeh, C. M. Allen, and T. Jaskoll, "Human cytomegalovirus and mucoepidermoid carcinoma of salivary glands: cell-specific localization of active viral and oncogenic signaling proteins is confirmatory of a causal relationship," *Experimental and Molecular Pathology*, vol. 92, no. 1, pp. 118–125, 2012.

[7] E. Dalpa, V. Gourvas, S. Baritaki et al., "High prevalence of human herpes virus 8 (HHV-8) in patients with Warthin's tumors of the salivary gland," *Journal of Clinical Virology*, vol. 42, no. 2, pp. 182–185, 2008.

[8] J. Kononen, L. Bubendorf, A. Kallioniemi et al., "Tissue microarrays for high-throughput molecular profiling of tumor specimens," *Nature Medicine*, vol. 4, no. 7, pp. 844–847, 1998.

[9] F. C.-F. Lin, P.-L. Chen, T.-Y. Tsao, C.-R. Li, K.-C. Jeng, and S. C.-S. Tsai, "Prevalence of human papillomavirus and Epstein–Barr virus in salivary gland diseases," *The Journal of International Medical Research*, vol. 42, no. 5, pp. 1093–1101, 2014.

[10] A. E. Rytkönen, P. P. Hirvikoski, and T. A. Salo, "Lymphoepithelial carcinoma: two case reports and a systematic review of oral and sinonasal cases," *Head and Neck Pathology*, vol. 5, no. 4, pp. 327–334, 2011.

[11] T. Terada, "Epstein-Barr virus associated lymphoepithelial carcinoma of the esophagus," *International Journal of Clinical and Experimental Medicine*, vol. 6, no. 3, pp. 219–226, 2013.

[12] L. A. Cerilli, V. A. Holst, M. S. Brandwein, M. H. Stoler, and S. E. Mills, "Sinonasal undifferentiated carcinoma: immunohistochemical profile and lack of EBV association," *The American Journal of Surgical Pathology*, vol. 25, no. 2, pp. 156–163, 2001.

[13] F. Dadmanesh, J. L. Peterse, A. Sapino, A. Fonelli, and V. Eusebi, "Lymphoepithelioma-like carcinoma of the breast: lack of evidence of Epstein-Barr virus infection," *Histopathology*, vol. 38, no. 1, pp. 54–61, 2001.

[14] S. Ferlicot, F. Plantier, L. Rethers, A. D. Bui, and J. Wechsler, "Lymphoepithelioma-like carcinoma of the skin: a report of 3 Epstein-Barr virus (EBV)-negative additional cases. Immunohistochemical study of the stroma reaction," *Journal of Cutaneous Pathology*, vol. 27, no. 6, pp. 306–311, 2000.

[15] J. Kulka, I. Kovalszky, E. Svastics, M. Berta, and T. Füle, "Lymphoepithelioma-like carcinoma of the breast: not Epstein-Barr virus-, but human papilloma virus-positive," *Human Pathology*, vol. 39, no. 2, pp. 298–301, 2008.

[16] E. Szekely, "Lymphoepithelioma-like cholangiocarcinoma (LELC) not associated with Epstein-Barr virus," *The American Journal of Surgical Pathology*, vol. 25, no. 11, pp. 1464–1466, 2001.

[17] J. C. Tardío, E. Cristóbal, F. Burgos, and J. Menárguez, "Absence of EBV genome in lymphoepithelioma-like carcinomas of the larynx," *Histopathology*, vol. 30, no. 2, pp. 126–128, 1997.

[18] T. Kuo and C. Hsueh, "Lymphoepithelioma-like salivary gland carcinoma in Taiwan: a clinicopathological study of nine cases demonstrating a strong association with Epstein-Barr virus," *Histopathology*, vol. 31, no. 1, pp. 75–82, 1997.

[19] C.-C. Tsai, C.-L. Chen, and H.-C. Hsu, "Expression of Epstein-Barr virus in carcinomas of major salivary glands: a strong association with lymphoepithelioma-like carcinoma," *Human Pathology*, vol. 27, no. 3, pp. 258–262, 1996.

[20] L. M. Weiss, L. A. Movahed, A. E. Butler et al., "Analysis of lymphoepithelioma and lymphoepithelioma-like carcinomas for Epstein-Barr viral genomes by in situ hybridization," *The American Journal of Surgical Pathology*, vol. 13, no. 8, pp. 625–631, 1989.

[21] T. Atula, R. Grénman, P. Klemi, and S. Syrjänen, "Human papillomavirus, Epstein-Barr virus, human herpesvirus 8 and human cytomegalovirus involvement in salivary gland tumours," *Oral Oncology*, vol. 34, no. 5, pp. 391–395, 1998.

[22] M. Santucci, O. Gallo, A. Calzolari, and R. Bondi, "Detection of Epstein-Barr viral genome in tumor cells of Warthin's tumor of parotid gland," *American Journal of Clinical Pathology*, vol. 100, no. 6, pp. 662–665, 1993.

[23] C. Casper, "The aetiology and management of Castleman disease at 50 years: translating pathophysiology to patient care," *British Journal of Haematology*, vol. 129, no. 1, pp. 3–17, 2005.

[24] W. Quinibi, O. Al-Furayh, K. Almeshari et al., "Serologic association of human herpesvirus eight with posttransplant Kaposi's sarcoma in Saudi Arabia," *Transplantation*, vol. 65, no. 4, pp. 583–585, 1998.

[25] R. G. Nador, E. Cesarman, A. Chadburn et al., "Primary effusion lymphoma: a distinct clinicopathologic entity associated with the Kaposi's sarcoma-associated herpes virus," *Blood*, vol. 88, no. 2, pp. 645–656, 1996.

[26] T. Rampias, C. Sasaki, P. Weinberger, and A. Psyrri, "E6 and E7 gene silencing and transformed phenotype of human papillomavirus 16-positive oropharyngeal cancer cells," *Journal of the National Cancer Institute*, vol. 101, no. 6, pp. 412–423, 2009.

[27] J. P. Klussmann, A. Müller, M. Wagner et al., "Human herpesvirus type 8 in salivary gland tumors," *Journal of Clinical Virology*, vol. 16, no. 3, pp. 239–246, 2000.

[28] D. J. Blackbourn, E. T. Lennette, J. Ambroziak, D. V. Mourich, and J. A. Levy, "Human herpesvirus 8 detection in nasal secretions and saliva," *Journal of Infectious Diseases*, vol. 177, no. 1, pp. 213–216, 1998.

[29] P. Cattani, M. Capuano, F. Cerimele et al., "Human herpesvirus 8 seroprevalence and evaluation of nonsexual transmission routes by detection of DNA in clinical specimens from human immunodeficiency virus-seronegative patients from central and southern Italy, with and without Kaposi's sarcoma," *Journal of Clinical Microbiology*, vol. 37, no. 4, pp. 1150–1153, 1999.

[30] M. E. McLaughlin-Drubin, C. P. Crum, and K. Münger, "Human papillomavirus E7 oncoprotein induces KDM6A and KDM6B histone demethylase expression and causes epigenetic reprogramming," *Proceedings of the National Academy of Sciences of the United States of America*, vol. 108, no. 5, pp. 2130–2135, 2011.

[31] R. L. Cantley, E. Gabrielli, F. Montebelli, D. Cimbaluk, P. Gattuso, and G. Petruzzelli, "Ancillary studies in determining human papillomavirus status of squamous cell carcinoma of the oropharynx: a review," *Pathology Research International*, vol. 2011, Article ID 138469, 7 pages, 2011.

[32] A. Skálová, J. Kapírková, P. Andrle, L. Hostička, and T. Vaneček, "Human papillomaviruses are not involved in the etiopathogenesis of salivary gland tumors," *Czecho-Slovak Pathology*, vol. 49, no. 2, pp. 72–75, 2013.

[33] T. Isayeva, N. Said-Al-Naief, Z. Ren, R. Li, D. Gnepp, and M. Brandwein-Gensler, "Salivary mucoepidermoid carcinoma: demonstration of transcriptionally active human papillomavirus 16/18," *Head and Neck Pathology*, vol. 7, no. 2, pp. 135–148, 2013.

[34] L. Hafed, H. Farag, O. Shaker, and D. El-Rouby, "Is human papilloma virus associated with salivary gland neoplasms? An in situ-hybridization study," *Archives of Oral Biology*, vol. 57, no. 9, pp. 1194–1199, 2012.

[35] E. Senft, J. Lemound, A. Stucki-Koch, N. Gellrich, H. Kreipe, and K. Hussein, "Expression of cyclin-dependent kinase inhibitor 2A 16, tumour protein 53 and epidermal growth factor receptor in salivary gland carcinomas is not associated with oncogenic virus infection," *International Journal of Oral Science*, vol. 7, no. 1, pp. 18–22, 2015.

[36] J. A. Bishop, R. Yonescu, D. Batista, A. Yemelyanova, P. K. Ha, and W. H. Westra, "Mucoepidermoid carcinoma does not harbor transcriptionally active high risk human papillomavirus even in the absence of the MAML2 translocation," *Head and Neck Pathology*, vol. 8, no. 3, pp. 298–302, 2014.

[37] G. Jour, K. West, V. Ghali, D. Shank, G. Ephrem, and B. M. Wenig, "Differential expression of $p16^{INK4A}$ and cyclin D1 in benign and malignant salivary gland tumors: a study of 44 cases," *Head and Neck Pathology*, vol. 7, no. 3, pp. 224–231, 2013.

[38] R. Herrero, X. Castellsagué, M. Pawlita et al., "Human papillomavirus and oral cancer: the international agency for research on cancer multicenter study," *Journal of the National Cancer Institute*, vol. 95, no. 23, pp. 1772–1783, 2003.

[39] J. P. Klussmann, S. J. Weissenborn, U. Wieland et al., "Prevalence, distribution, and viral load of human papillomavirus 16 DNA in tonsillar carcinomas," *Cancer*, vol. 92, no. 11, pp. 2875–2884, 2001.

[40] R. D. M. Steenbergen, P. J. F. Snijders, D. A. M. Heideman, and C. J. L. M. Meijer, "Clinical implications of (epi)genetic changes in HPV-induced cervical precancerous lesions," *Nature Reviews Cancer*, vol. 14, no. 6, pp. 395–405, 2014.

[41] M. Schiffman, S. Boyle, T. Raine-Bennett et al., "The role of human papillomavirus genotyping in cervical cancer screening: a large-scale evaluation of the cobas HPV test," *Cancer Epidemiology, Biomarkers & Prevention*, vol. 24, no. 9, pp. 1304–1310, 2015.

[42] G. Campisi and L. Giovannelli, "Controversies surrounding human papilloma virus infection, head & neck vs oral cancer, implications for prophylaxis and treatment," *Head & Neck Oncology*, vol. 1, article 8, 2009.

[43] H. Riechelmann, "Humane papillomaviren bei Kopf-Hals-Karzinomen," *Laryngo-Rhino-Otologie*, no. 89, pp. 43–48, 2010.

[44] E. Daley, V. Dodd, R. DeBate et al., "Prevention of HPV-related oral cancer: assessing dentists' readiness," *Public Health*, vol. 128, no. 3, pp. 231–238, 2014.

[45] M. L. Gillison, A. K. Chaturvedi, and D. R. Lowy, "HPV prophylactic vaccines and the potential prevention of noncervical cancers in both men and women," *Cancer*, vol. 113, no. 10, pp. 3036–3046, 2008.

[46] A. B. Ryerson, E. S. Peters, S. S. Coughlin et al., "Burden of potentially human papillomavirus-associated cancers of the oropharynx and oral cavity in the US, 1998–2003," *Cancer*, vol. 113, no. 10, pp. 2901–2909, 2008.

Hindawi Publishing Corporation
BioMed Research International
Volume 2015, Article ID 839403, 7 pages
http://dx.doi.org/10.1155/2015/839403

Research Article

Clinical Significance of Cannabinoid Receptors CB1 and CB2 Expression in Human Malignant and Benign Thyroid Lesions

Eleftheria Lakiotaki,[1] Constantinos Giaginis,[1,2] Maria Tolia,[3] Paraskevi Alexandrou,[1] Ioanna Delladetsima,[1] Ioanna Giannopoulou,[1] George Kyrgias,[3] Efstratios Patsouris,[1] and Stamatios Theocharis[1]

[1]*First Department of Pathology, Medical School, University of Athens, Athens, Greece*
[2]*Department of Food Science and Nutrition, University of the Aegean, Myrina, Lemnos, Greece*
[3]*Department of Radiotherapy, School of Health Sciences, Faculty of Medicine, University of Thessaly, Larissa, Greece*

Correspondence should be addressed to Maria Tolia; martolia@med.uoa.gr

Received 1 June 2015; Accepted 11 August 2015

Academic Editor: Monica Cantile

The endocannabinoid system is comprised of cannabinoid receptors (CB1 and CB2), their endogenous ligands (endocannabinoids), and proteins responsible for their metabolism participate in many different functions indispensable to homeostatic regulation in several tissues, exerting also antitumorigenic effects. The present study aimed to evaluate the clinical significance of CB1 and CB2 expression in human benign and malignant thyroid lesions. CB1 and CB2 proteins' expression was assessed immunohistochemically on paraffin-embedded thyroid tissues obtained from 87 patients with benign ($n = 43$) and malignant ($n = 44$) lesions and was statistically analyzed with clinicopathological parameters, follicular cells' proliferative capacity, and risk of recurrence rate estimated according to the American Thyroid Association (ATA) staging system. Enhanced CB1 and CB2 expression was significantly more frequently observed in malignant compared to benign thyroid lesions ($p = 0.0010$ and $p = 0.0005$, resp.). Enhanced CB1 and CB2 expression was also significantly more frequently observed in papillary carcinomas compared to hyperplastic nodules ($p = 0.0097$ and $p = 0.0110$, resp.). In malignant thyroid lesions, elevated CB2 expression was significantly associated with the presence of lymph node metastases ($p = 0.0301$). Enhanced CB2 expression was also more frequently observed in malignant thyroid cases with presence of capsular ($p = 0.1165$), lymphatic ($p = 0.1989$), and vascular invasion ($p = 0.0555$), as well as in those with increased risk of recurrence rate ($p = 0.1165$), at a nonsignificant level though, whereas CB1 expression was not associated with any of the clinicopathological parameters examined. Our data suggest that CB receptors may be involved in malignant thyroid transformation and especially CB2 receptor could serve as useful biomarker and potential therapeutic target in thyroid neoplasia.

1. Introduction

Endocannabinoid system (ECS) is an endogenous lipid signal-inducing system, present in various human tissues, that exerts many different and unrelated functions. Substantial studies have indicated the regulatory effects of the ECS on the central and peripheral nervous system, the gastrointestinal tract, and the immune system, being involved in multiple processes, such as gastrointestinal motility, mood, pain regulation, memory, and appetite [1]. These functions are triggered by binding of endogenous and exogenous ligands to cannabinoid receptors (CB receptors). Besides those well-known functions, ECS also exerts antiproliferative effects through modulation of several signaling pathways [2], while its activation may have prognostic significance for tumor developmental progression [3–6].

Two subtypes of CB receptors exist, with different distribution among the human tissues. CB1 receptor is mainly located at the central nervous system, adipocytes, liver, pancreas, skeletal muscle, and T-lymphocytes [7]. CB2 receptor

is mainly detected in immune cells, but also in neurons and other cells that comprise the central nervous system such as astrocytes and microglia as well as in cerebromicrovascular endothelial cells [8]. The activation of CB receptors inhibits cAMP formation through its coupling to Gi proteins, resulting in decreased protein kinase A- (PKA-) dependent phosphorylation [7, 8]. CB receptors also couple to extracellular signal-regulated kinase (ERK) and specifically p42/p44 and p38 [2], participating in phosphatidylinositol 3-kinase (PI3K) and ceramide signaling [9]. Other receptors are also attached to the ECS like transient receptor potential cation channel subfamily V member 1 (TRPV-1), peroxisome proliferator-activated receptors (PPARs), and non-CB1/CB2 G-protein-coupled receptors GPR55 [7, 8].

The ECS ligands are the cannabinoids, including the bioactive components of the Cannabis Sativa, synthetic CB-mimetic compounds, and endogenous ligands of CB receptors [10]. The most important molecule of the first category is Δ^9-THC, which is well known for its psychoactive traits [10]. The other two categories include synthetic ligands that have currently been developed (CP55940, HU-210, HU-211, ab-cannabidiol, ajulemic acid, WIN55,212-2) and endocannabinoids that are produced by the human body and are lipid messenger derivatives of arachidonic acid (AA) conjugated with either ethanolamine or glycerol [11]. The most important of these molecules are anandamide (AEA) and 2-arachidonoylglycerol (2-AG), but additional substances have also been identified, such as O-arachidonoylethanolamine (OAE, virodhamine), 2-arachidonoylglycerol ether (2-AGE, noladin ether), N-arachidonoyldopamine (NADA), and palmitoylethanolamide (PEA) [10, 11]. Apart from the CB receptors and all their ligands, the ECS also includes the essential enzymes for ligand biosynthesis, transport, and degradation [8, 10, 11].

In addition to ECS functions in order to maintain homeostasis, the above-mentioned cross-talk between the ECS and the most important oncogenic pathways (MAPK/ERK and PI3K/Akt pathway) has recently gained interest and has highlighted the significance of the ECS in tumorigenesis [12, 13]. Moreover, cannabinoids have been shown to induce apoptosis in cancer cells, inhibit tumor vascularization via VEGF decrease, and suppress cancer cell invasive capacity [12, 13]. Antiproliferative effects prevail and several studies suggest that cannabinoids have potential as antitumoral agents [12, 13].

Diagnosis of thyroid lesions has recently been increased, not only due to improved diagnostic techniques, but also because of their true incidence rise in the population [14]. In fact, thyroid carcinoma is the most common malignancy of the endocrine system [14]. Although thyroid cancer is usually completely cured by surgery and therapy, 10–20% of patients still die from recurrence or tumor progression [15]. Therefore, it is essential to establish new treatment strategies and find new prognostic markers in order to predict the clinical course for each patient and customize accordingly the available therapeutic modalities. In this aspect, the present study aimed to evaluate the immunohistochemical expression of CB1 and CB2 receptor in benign and malignant thyroid lesions in association with clinicopathological characteristics related to prognosis.

2. Patients and Methods

2.1. Patients. The examined material consisted of 87 histologically examined thyroid surgical specimens from an equal number of patients who had undergone thyroid surgery for benign and malignant lesions. Forty-three benign (37 hyperplastic nodules and 6 Hashimoto thyroiditis) and forty-four malignant (40 papillary and 4 follicular carcinomas) cases were included in the study. Each neoplasm was classified according to the WHO histological classification of thyroid tumors [16]. The risk of recurrence was estimated according to the American Thyroid Association (ATA) staging system [17]. None of the patients had received any kind of anticancer treatment prior to surgery and there was no clinical history of head and neck irradiation or of other cancer.

2.2. Immunohistochemistry. Immunostainings for CB1 and CB2 were performed on formalin-fixed, paraffin-embedded thyroid tissue sections using a goat polyclonal CB1 IgG antibody (N-15, sc-10066, Santa Cruz Biotechnology, Santa Cruz, CA, USA) and a rabbit polyclonal CB2 IgG antibody (H-60, sc-25494, Santa Cruz Biotechnology). Briefly, 4 μm thick tissue sections were dewaxed in xylene and were brought to water through graded alcohols. Antigen retrieval was performed by microwaving slides in 10 mM citrate buffer (pH 6.1) for 15 minutes (min) at high power, according to the manufacturer's instructions. To remove the endogenous peroxidase activity, sections were then treated with freshly prepared 0.3% hydrogen peroxide in methanol in the dark, for 30 min, at room temperature. Nonspecific antibody binding was blocked using Eraser and Sniper, specific blocking reagents for goat and rabbit primary antibodies, respectively (Biocare Medical, Concord, California, USA), for 5 min. The sections were incubated for 1 hour (h), at room temperature, with the primary antibodies against CB1 and CB2 diluted 1 : 300 and 1 : 200, respectively, in phosphate buffered saline (PBS) according to the manufacturer's instructions. Sections were then incubated at room temperature with biotinylated linking reagent (Biocare Medical) for 10 min, followed by incubation with peroxidase-conjugated streptavidin label (Biocare Medical) for 10 min. The resultant immune peroxidase activity was developed using a DAB substrate kit (Vector Laboratories, California, USA) for 10 min. Sections were counterstained with Harris' hematoxylin and mounted in Entellan (Merck, Darmstadt, Germany). Appropriate negative controls were performed by omitting the primary antibody and/or substituting it with an irrelevant antiserum. As positive control, breast and mobile tongue squamous cell carcinoma tissue sections with known CB1 and CB2 expression were used. The follicular cells' proliferative capacity was assessed by Ki-67 immunohistochemical expression, as previously described [18–20].

2.3. Evaluation of Immunohistochemistry. Immunohistochemical evaluation was performed by counting at least 1000

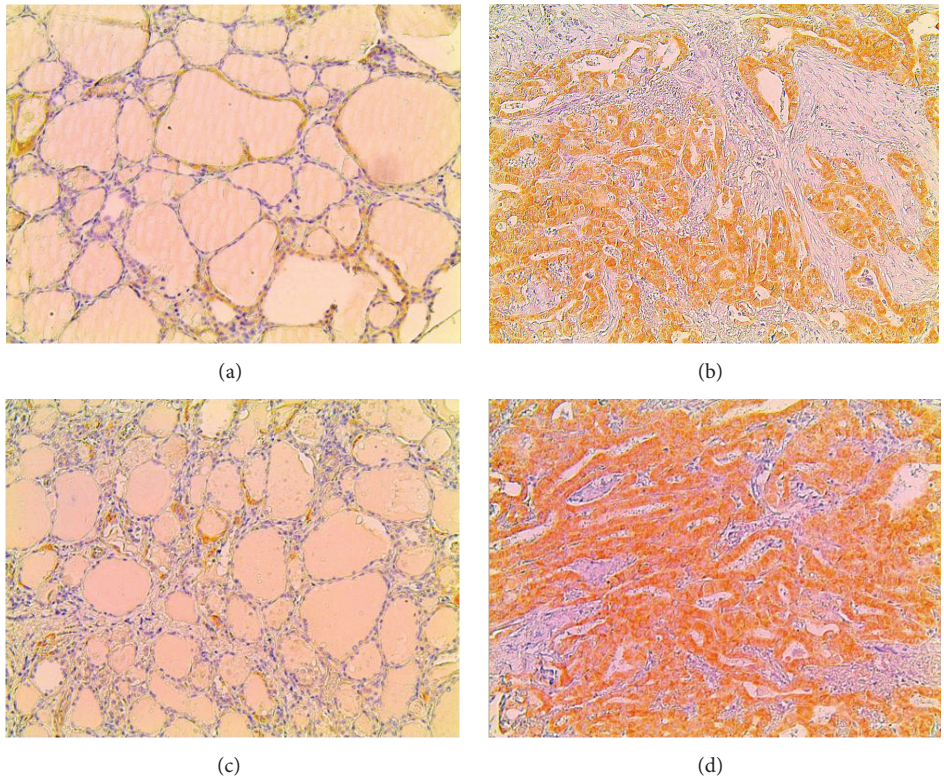

(a) (b) (c) (d)

Figure 1: Representative CB1 immunostainings in: (a) hyperplastic nodule and (b) papillary carcinoma. Representative CB2 immunostainings in (c) hyperplastic nodule and (d) papillary carcinoma (original magnification ×200).

tumour cells in each case by two independent observers (Stamatios Theocharis and Paraskevi Alexandrou) blinded to the clinical data, with complete observer agreement. Specimens were considered "positive" for CB1 and CB2 when more than 5% of tumour cells within the section were positively stained [18–20]. The immunoreactivity of the tumor cells for CB1 and CB2 was scored according to the percentage of CB1 and CB2 positive tumor cells as 0: negative staining- 0–4% of tumor cells positive; 1: 5–24% of tumor cells positive; 2: 25–49% of tumor cells positive; 3: 50–100% of tumor cells positive and its intensity as 0: negative staining, 1: mild staining; 2: intermediate staining; 3: intense staining [18–20]. Finally, the expression of CB1 and CB2 was classified as low, if the total score was 0 or 2 and high and if the total score was ≥3 [18–20]. Ki-67 immunoreactivity was classified according to the percentage of positively stained follicular cells exceeded the median percentage value into two categories (below and over mean value), as previously reported [18–20].

2.4. Statistical Analysis. Chi-square tests were used to assess the difference of CB1 and CB2 expression between malignant and benign thyroid lesions, as well as between papillary carcinoma cases and hyperplastic nodules. Chi-square tests were applied to assess the associations between CB1 and CB2 expression and clinicopathological characteristics in the subgroup of patients with malignant thyroid lesions. A 2-tailed $p < 0.05$ was considered statistically significant. Statistical analyses were performed using the software package SPSS for Windows (version 13.0; SPSS Inc., Chicago, IL, USA).

3. Results

3.1. Clinical Significance of CB1 Expression in Human Malignant and Benign Thyroid Lesions. CB1 positivity (IHC score > 0) was noted in 52 (60%) out of 87 thyroid lesions. Thirty-one (36%) out of the 87 examined cases presented high CB1 immunoreactivity (IHC score ≥ 3). The subcellular pattern of CB1 distribution was predominantly cytoplasmic and occasionally membranous. Normal surrounding areas adjacent to tumour were found negative for CB1. Representative CB1 immunostainings for hyperplastic nodule and papillary carcinoma are depicted in Figures 1(a) and 1(b), respectively. CB1 immunoreactivity was significantly different between benign and malignant thyroid lesions (Table 1, $p = 0.0010$). High CB1 expression was significantly more frequently observed in papillary carcinoma compared to hyperplastic nodules (Table 1, $p = 0.0097$). CB1 expression was not associated to patients' age and gender and follicular cells' proliferative capacity. In the subgroup of malignant thyroid lesions, high CB1 expression was noted in 23 (52%) out of 44 cases. There was no association between CB1 receptor expression and tumour size, presence of capsular, vascular or lymphatic invasion, lymph node metastasis, and follicular cells' proliferation rate (Table 2). CB1 receptor expression was not associated with risk of recurrence estimated according to ATA staging system (data not shown).

3.2. Clinical Significance of CB2 Expression in Human Malignant and Benign Thyroid Lesions. CB2 positivity (IHC score

Table 1: Associations of CB1 and CB2 expression with patients' age and gender, type of histopathology, and Ki-67 protein statement in 87 patients with thyroid lesions.

Clinicopathological characteristics	CB1 expression			CB2 expression		
	Low	High	p value	Low	High	p value
$N = 87$	56 (64%)	31 (36%)		55 (63%)	32 (37%)	
Age (mean ± SD; yrs)	51.9 ± 14.2	49.5 ± 14.3	0.4584	50.7 ± 14.0	51.7 ± 14.7	0.7620
Gender			0.5470			0.6068
Female	46 (53%)	27 (31%)		47 (54%)	26 (30%)	
Male	10 (11%)	4 (5%)		8 (9%)	6 (7%)	
Histopathology ($N = 87$)			0.0010			0.0005
Benign	35 (40%)	8 (10%)		35 (40%)	8 (9%)	
Malignant	21 (24%)	23 (26%)		20 (23%)	24 (28%)	
Histopathology ($N = 77$)			0.0097			0.0110
Hyperplastic nodules	29 (38%)	8 (10%)		30 (39%)	7 (9%)	
Papillary carcinoma	20 (26%)	20 (26%)		18 (23%)	22 (29%)	
Ki-67 protein statement			0.5051			0.3087
Below mean value	45 (52%)	23 (26%)		47 (54%)	21 (24%)	
Over mean value	11 (12%)	8 (10%)		8 (9%)	11 (13%)	

Table 2: Associations of CB1 and CB2 expression with clinicopathological characteristics in 44 patients with malignant thyroid lesions.

Clinicopathological characteristics	CB1 expression			CB2 expression		
	Low	High	p value	Low	High	p value
$N = 44$	21 (48%)	23 (52%)		20 (45%)	24 (55%)	
Age (mean ± SD; yrs)	51.2 ± 14.4	50.1 ± 14.6		50.2 ± 13.8	51.3 ± 14.9	0.7201
Gender			0.2021			0.9456
Female	15 (34%)	20 (45%)		16 (36%)	19 (43%)	
Male	6 (14%)	3 (7%)		4 (9%)	5 (12%)	
Tumor size (T)			0.6011			0.4844
T1	15 (34%)	18 (41%)		16 (36%)	17 (39%)	
T2–4	6 (14%)	5 (11%)		4 (9%)	7 (16%)	
Lymph node metastasis (N)			0.7132			0.0301
N0	19 (43%)	20 (45%)		20 (45%)	19 (43%)	
N1	2 (5%)	3 (7%)		0 (0%)	5 (12%)	
Capsular invasion			0.8250			0.1165
No	17 (39%)	18 (41%)		18 (41%)	17 (39%)	
Yes	4 (9%)	5 (11%)		2 (4%)	7 (16%)	
Lymphatic invasion			0.5220			0.1989
No	18 (41%)	18 (41%)		18 (41%)	18 (41%)	
Yes	3 (7%)	5 (11%)		2 (4%)	6 (14%)	
Vascular invasion			0.3398			0.0555
No	20 (45%)	20 (45%)		20 (45%)	20 (45%)	
Yes	1 (3%)	3 (7%)		0 (0%)	4 (10%)	
Ki-67 protein statement			0.5827			0.2828
Below mean value	12 (27%)	15 (34%)		14 (32%)	13 (30%)	
Over mean value	9 (21%)	8 (18%)		6 (14%)	11 (25%)	

> 0) was noted in 61 (71%) out of 87 thyroid lesions. Thirty-two (37%) out of the 87 examined cases presented high CB2 immunoreactivity (IHC score ≥ 3). The subcellular pattern of distribution was predominantly cytoplasmic and occasionally membranous. Normal surrounding areas adjacent to tumor were found negative for CB2. Representative CB2 immunostainings for hyperplastic nodules and papillary carcinoma are depicted in Figures 1(c) and 1(d), respectively. High CB2 expression was significantly more frequently observed in malignant thyroid lesions compared to benign ones, as well

as in papillary carcinoma compared to hyperplastic nodules (Table 1, $p = 0.0005$ and $p = 0.0110$, resp.). In the subgroup of malignant thyroid lesions, high CB2 expression was noted in 24 (55%) out of 44 cases. High CB2 expression was significantly associated with the presence of lymph node metastasis (Table 2, $p = 0.0301$). High CB2 expression was also associated with the presence of capsular, lymphatic invasion, and vascular invasion, at a nonsignificant level though (Table 2, $p = 0.1165$, $p = 0.1989$, and $p = 0.0555$, resp.). No associations between CB2 expression and patients' age and gender, tumour size, and follicular cells' proliferative rate were noted (Table 2). High CB2 receptor expression was more frequently observed in malignant thyroid lesions presenting increased risk of recurrence rate according to ATA staging system, at a nonsignificant level though ($p = 0.1165$).

4. Discussion

In the present study, CB1 and CB2 protein expression was increased in malignant compared to benign thyroid lesions. We also describe for the first time an association between CB2 protein expression and clinicopathological parameters crucial for patients' management and prognosis. Notably, enhanced CB2 expression was significantly associated with the presence of lymph node metastases and borderline with the presence of vascular invasion, while indicative but nonsignificant associations with the presence of capsular and lymphatic invasion and estimated recurrence rate were also noted. Similar results for CB1 receptor overexpression were obtained, as far as malignant compared to benign thyroid lesions are concerned; nevertheless nonsignificant association or trend of correlation between CB1 expression and clinicopathological parameters was noted.

In accordance with the present findings, CB receptors were upregulated in certain tumour human malignancies, including oral squamous cell carcinoma, pancreatic, hepatocellular, and prostatic carcinoma, whereas they were not expressed in normal tissues of these organs [3–6]. On the other hand, CB1 receptor was downregulated in colorectal carcinoma in contrast to adjacent normal tissues, pointing to the different roles of the ECS in various tumors and indicating the multiple interactions between the ECS and the mechanisms that control cell growth and proliferation [21]. These mechanisms may include direct induction of transformed-cell death, cell cycle arrest, and inhibition of tumor angiogenesis and metastasis [12, 13]. The antitumoral effects of ECS have also been depicted in numerous studies. In colorectal cancer, endocannabinoids and synthetic cannabinoids were able to induce apoptosis and inhibit carcinogenesis by mechanisms involving both CB receptors, TRPV1 channels and PPARγ-pathway [22, 23]. Similar results have occurred in studies conducted on pancreatic, lung, and breast cancer, cholangiocarcinoma, and hepatocellular carcinoma [24–28]. Synergistic effects of cannabinoids with conventional antitumor chemotherapy have also been reported [29].

CB receptor overexpression in thyroid carcinoma has recently been reported, *in vitro* [30, 31]. More to the point, IL-12 stimulation of anaplastic thyroid carcinoma cell lines induced CB2 receptor overexpression and led to CB2-agonist mediated apoptosis and tumour regression [30]. Moreover, CB2 upregulation rendered the tumour cells more susceptible to treatment with standard chemotherapy [30]. One putative explanation for this phenomenon was the ceramide-dependent activation of the mitochondrial intrinsic pathway, which leads to apoptosis, being triggered by CB2 receptor activation [32]. Another study on thyroid carcinoma cell lines depicted that 2-methyl-2′-F-anandamide (Met-F-AEA) inhibited tumour growth, associated with high CB1 receptor levels [31]. The abundant CB1 receptor expression was noted in more responsive to treatment cell lines, which subsequently were more susceptible to growth inhibition. Such results were ascribed to p53 activation, $p21^{CIP1/WAF1}$ increase, and cyclin A decrease, leading to apoptosis [31].

Apart from the possible therapeutic implications concerning tumorigenesis and ECS, detection of CB receptors overexpression may have potential as prognostic indicators. Upregulation of both CB receptors in hepatocellular carcinoma tissue samples was significantly associated with improved prognosis and longer disease-free survival [3]. Such findings were combined with the histopathological tumour characteristics, as high CB receptor levels were observed in cases presenting well differentiation and limited portal tract involvement [3]. On the other hand, CB2 immunoreactivity was associated with shorter disease-free survival in head and neck squamous cell carcinoma [6]. Concerning CB1 receptor, its overexpression was associated with poor patients' outcome in colorectal, prostatic, and pancreatic carcinoma [4, 5, 21]. Notably, enhanced CB1 expression in stage IV colorectal carcinoma patients was independently correlated with poor prognosis [21]. Increased CB1 expression was also associated with aggressive prostatic adenocarcinoma presenting higher Gleason score, larger tumour size, and increased cell proliferation rate, as well as metastasis at diagnosis [5]. Moreover, low CB1 expression or high FAAH/MAGL levels were correlated with longer survival rate and higher pain status. Similar but not statistically significant results for CB2 receptor were noted [4]. Taking into account the above mentioned data, the currently available studies on CB receptor levels and their associations with prognosis in various tumors seem contradictory and may be closely related to the extent of ECS participation in tumorigenesis.

5. Conclusion

Enhanced CB1 and CB2 receptor immunohistochemical expression levels were correlated with thyroid gland malignancy. Moreover, enhanced CB2 expression levels were associated with clinicopathological characteristics important for patients' therapeutic management. These results supported evidence that CB receptors and especially CB2 receptor may interfere with molecular pathways participating in thyroid malignant transformation and could be considered as potential therapeutic targets to suppress tumor progression. Larger cohort studies are strongly recommended in order to confirm and establish the clinical utility of CB receptors as potential prognostic markers in thyroid neoplasia.

Conflict of Interests

All authors verify that they have not accepted any funding or support from an organization that may in any way gain or lose financially from the results of the present study. All authors verify that they have not been employed by an organization that may in any way gain or lose financially from the results of the present study. None of the authors have any other conflict of interests.

Authors' Contribution

Eleftheria Lakiotaki and Constantinos Giaginis contributed equally to the study.

References

[1] A. A. Izzo and K. A. Sharkey, "Cannabinoids and the gut: new developments and emerging concepts," *Pharmacology and Therapeutics*, vol. 126, no. 1, pp. 21–38, 2010.

[2] P. Derkinderen, C. Ledent, M. Parmentier, and J.-A. Girault, "Cannabinoids activate p38 mitogen-activated protein kinases through CB1 receptors in hippocampus," *Journal of Neurochemistry*, vol. 77, no. 3, pp. 957–960, 2001.

[3] X. Xu, Y. Liu, S. Huang et al., "Overexpression of cannabinoid receptors CB1 and CB2 correlates with improved prognosis of patients with hepatocellular carcinoma," *Cancer Genetics and Cytogenetics*, vol. 171, no. 1, pp. 31–38, 2006.

[4] C. W. Michalski, F. E. Oti, M. Erkan et al., "Cannabinoids in pancreatic cancer: correlation with survival and pain," *International Journal of Cancer*, vol. 122, no. 4, pp. 742–750, 2008.

[5] S. C. Chung, P. Hammarsten, A. Josefsson et al., "A high cannabinoid CB1 receptor immunoreactivity is associated with disease severity and outcome in prostate cancer," *European Journal of Cancer*, vol. 45, no. 1, pp. 174–182, 2009.

[6] T. J. W. Klein Nulent, P. J. Van Diest, P. van der Groep et al., "Cannabinoid receptor-2 immunoreactivity is associated with survival in squamous cell carcinoma of the head and neck," *British Journal of Oral and Maxillofacial Surgery*, vol. 51, no. 7, pp. 604–609, 2013.

[7] L. K. Miller and L. A. Devi, "The highs and lows of cannabinoid receptor expression in disease: mechanisms and their therapeutic implications," *Pharmacological Reviews*, vol. 63, no. 3, pp. 461–470, 2011.

[8] R. G. Pertwee, A. C. Howlett, M. E. Abood et al., "International Union of Basic and Clinical Pharmacology. LXXIX. Cannabinoid receptors and their ligands: beyond CB_1 and CB_2," *Pharmacological Reviews*, vol. 62, no. 4, pp. 588–631, 2010.

[9] E. Molina-Holgado, J. M. Vela, A. Arévalo-Martín et al., "Cannabinoids promote oligodendrocyte progenitor survival: involvement of cannabinoid receptors and phosphatidylinositol-3 kinase/Akt signaling," *The Journal of Neuroscience*, vol. 22, no. 22, pp. 9742–9753, 2002.

[10] L. De Petrocellis and V. Di Marzo, "An introduction to the endocannabinoid system: from the early to the latest concepts," *Best Practice and Research: Clinical Endocrinology and Metabolism*, vol. 23, no. 1, pp. 1–15, 2009.

[11] V. Di Marzo and L. De Petrocellis, "Why do cannabinoid receptors have more than one endogenous ligand?" *Philosophical Transactions of the Royal Society B: Biological Sciences*, vol. 367, no. 1607, pp. 3216–3228, 2012.

[12] S. Pisanti, P. Picardi, A. D'Alessandro, C. Laezza, and M. Bifulco, "The endocannabinoid signaling system in cancer," *Trends in Pharmacological Sciences*, vol. 34, no. 5, pp. 273–282, 2013.

[13] R. Van Dross, E. Soliman, S. Jha, T. Johnson, and S. Mukhopadhyay, "Receptor-dependent and receptor-independent endocannabinoid signaling: a therapeutic target for regulation of cancer growth," *Life Sciences*, vol. 92, no. 8-9, pp. 463–466, 2013.

[14] E. M. Ward, A. Jemal, and A. Chen, "Increasing incidence of thyroid cancer: is diagnostic scrutiny the sole explanation?" *Future Oncology*, vol. 6, no. 2, pp. 185–188, 2010.

[15] H. Gharib and E. Papini, "Thyroid nodules: clinical importance, assessment, and treatment," *Endocrinology and Metabolism Clinics of North America*, vol. 36, no. 3, pp. 707–735, 2007.

[16] J. Rosai, "Appendix C. staging of cancer," in *Rosai and Ackerman's Surgical Pathology*, M. Houston, Ed., pp. 2809–2810, Mosby, London, UK, 9th edition, 2004.

[17] R. M. Tuttle, H. Tala, J. Shah et al., "Estimating risk of recurrence in differentiated thyroid cancer after total thyroidectomy and radioactive iodine remnant ablation: using response to therapy variables to modify the initial risk estimates predicted by the new American thyroid association staging system," *Thyroid*, vol. 20, no. 12, pp. 1341–1349, 2010.

[18] C. Giaginis, P. Alexandrou, I. Delladetsima, I. Giannopoulou, E. Patsouris, and S. Theocharis, "Clinical significance of histone deacetylase (HDAC)-1, HDAC-2, HDAC-4, and HDAC-6 expression in human malignant and benign thyroid lesions," *Tumor Biology*, vol. 35, no. 1, pp. 61–71, 2014.

[19] C. Giaginis, C. Michailidi, V. Stolakis et al., "Expression of DNA repair proteins MSH2, MLH1 and MGMT in human benign and malignant thyroid lesions: an immunohistochemical study," *Medical Science Monitor*, vol. 17, no. 3, pp. BR81–BR90, 2011.

[20] C. Michailidi, C. Giaginis, V. Stolakis et al., "Evaluation of FAK and src expression in human benign and malignant thyroid lesions," *Pathology and Oncology Research*, vol. 16, no. 4, pp. 497–507, 2010.

[21] C. K. Jung, W. K. Kang, J. M. Park et al., "Expression of the cannabinoid type I receptor and prognosis following surgery in colorectal cancer," *Oncology Letters*, vol. 5, no. 3, pp. 870–876, 2013.

[22] G. Aviello, B. Romano, F. Borrelli et al., "Chemopreventive effect of the non-psychotropic phytocannabinoid cannabidiol on experimental colon cancer," *Journal of Molecular Medicine*, vol. 90, no. 8, pp. 925–934, 2012.

[23] B. Romano, F. Borrelli, E. Pagano, M. G. Cascio, R. G. Pertwee, and A. A. Izzo, "Inhibition of colon carcinogenesis by a standardized *Cannabis sativa* extract with high content of cannabidiol," *Phytomedicine*, vol. 21, no. 5, pp. 631–639, 2014.

[24] A. Carracedo, M. Gironella, M. Lorente et al., "Cannabinoids induce apoptosis of pancreatic tumor cells via endoplasmic reticulum stress-related genes," *Cancer Research*, vol. 66, no. 13, pp. 6748–6755, 2006.

[25] A. Preet, Z. Qamri, M. W. Nasser et al., "Cannabinoid receptors, CB1 and CB2, as novel targets for inhibition of non–small cell lung cancer growth and metastasis," *Cancer Prevention Research*, vol. 4, no. 1, pp. 65–75, 2011.

[26] C. Grimaldi, S. Pisanti, C. Laezza et al., "Anandamide inhibits adhesion and migration of breast cancer cells," *Experimental Cell Research*, vol. 312, no. 4, pp. 363–373, 2006.

[27] L. Huang, J. C. Ramirez, G. A. Frampton et al., "Anandamide exerts its antiproliferative actions on cholangiocarcinoma by activation of the GPR55 receptor," *Laboratory Investigation*, vol. 91, no. 7, pp. 1007–1017, 2011.

[28] O. Pellerito, G. Calvaruso, P. Portanova et al., "The synthetic cannabinoid WIN 55,212-2 sensitizes hepatocellular carcinoma cells to tumor necrosis factor-related apoptosis-inducing ligand (TRAIL)-induced apoptosis by activating p8/CCAAT/enhancer binding protein homologous protein (CHOP)/death receptor 5 (DR5) axis," *Molecular Pharmacology*, vol. 77, no. 5, pp. 854–863, 2010.

[29] S. B. Gustafsson, T. Lindgren, M. Jonsson, and S. O. P. Jacobsson, "Cannabinoid receptor-independent cytotoxic effects of cannabinoids in human colorectal carcinoma cells: synergism with 5-fluorouracil," *Cancer Chemotherapy and Pharmacology*, vol. 63, no. 4, pp. 691–701, 2009.

[30] Y. Shi, M. Zou, E. Y. Baitei et al., "Cannabinoid 2 receptor induction by IL-12 and its potential as a therapeutic target for the treatment of anaplastic thyroid carcinoma," *Cancer Gene Therapy*, vol. 15, no. 2, pp. 101–107, 2008.

[31] R. Cozzolino, G. Calì, M. Bifulco, and P. Laccetti, "A metabolically stable analogue of anandamide, Met-F-AEA, inhibits human thyroid carcinoma cell lines by activation of apoptosis," *Investigational New Drugs*, vol. 28, no. 2, pp. 115–123, 2010.

[32] B. Herrera, A. Carracedo, M. Diez-Zaera, T. Gómez del Pulgar, M. Guzmán, and G. Velasco, "The CB2 cannabinoid receptor signals apoptosis via ceramide-dependent activation of the mitochondrial intrinsic pathway," *Experimental Cell Research*, vol. 312, no. 11, pp. 2121–2131, 2006.

Hindawi Publishing Corporation
BioMed Research International
Volume 2015, Article ID 629754, 10 pages
http://dx.doi.org/10.1155/2015/629754

Research Article

Effect of Laryngeal Squamous Cell Carcinoma Tissue Implantation on the Chick Embryo Chorioallantoic Membrane: Morphometric Measurements and Vascularity

Virgilijus Uloza,[1] Alina Kuzminienė,[1] Sonata Šalomskaitė-Davalgienė,[2] Jolita Palubinskienė,[2] Ingrida Balnytė,[2] Ingrida Ulozienė,[1] Viktoras Šaferis,[3] and Angelija Valančiūtė[2]

[1]*Department of Otorhinolaryngology, Lithuanian University of Health Sciences, LT-50009 Kaunas, Lithuania*
[2]*Department of Histology and Embryology, Lithuanian University of Health Sciences, LT-50009 Kaunas, Lithuania*
[3]*Department of Physics, Mathematics and Biophysics, Lithuanian University of Health Sciences, LT-50009 Kaunas, Lithuania*

Correspondence should be addressed to Alina Kuzminienė; alinakuzminiene@gmail.com

Received 10 July 2015; Revised 9 September 2015; Accepted 10 September 2015

Academic Editor: Monica Cantile

Background. The aim of this study was to develop chick embryo chorioallantoic membrane (CAM) model of laryngeal squamous cell carcinoma (LSCC) and to evaluate the morphological and morphometric characteristics and angiogenic features of it. *Methods*. Fresh LSCC tissue samples obtained from 6 patients were implanted onto 15 chick embryo CAMs. Morphological, morphometric, and angiogenic changes in the CAM and chorionic epithelium were evaluated up to 4 days after the tumor implantation. Immunohistochemical analysis (34βE12, CD31, and Ki67 staining) was performed to detect cytokeratins and tumor endothelial cells and to evaluate the proliferative capacity of the tumor before and after implantation on the CAM. *Results*. The implanted LSCC tissue samples survived on the CAM in all the experiments and retained the essential morphologic characteristics and proliferative capacity of the original tumor. Implants induced thickening of both the CAM (103–417%, $p = 0.0001$) and the chorionic epithelium (70–140%, $p = 0.0001$) and increase in number of blood vessels (75–148%, $p = 0.0001$) in the CAM. *Conclusions*. This study clarifies that chick embryo CAM is a relevant assay for implanting LSCC tissue and provides the first morphological and morphometric characterization of the LSCC CAM model that opens new perspectives to study this disease.

1. Introduction

Laryngeal squamous cell carcinoma (LSCC) is one of the most common malignant tumors of the respiratory tract with an estimated incidence rate of 10/100 000 cases in males in Europe [1]. The overall 5-year survival of patients with this carcinoma localization in Europe was 63% in the period of 1995 to 2003. Despite the up-to-date treatment using advanced chemoradiation therapy and modern surgical techniques, the survival rate is not increasing remarkably within the last 30 years [1].

A better understanding of the biological mechanisms that control progression of LSCC would provide new and more successful strategies for tumor management. However, current *in vivo* models for human LSCC investigation do not simulate enough tumorigenic phenotypes of cancer and data about experimental evaluation of carcinogenesis, angiogenesis, and metastatic potential of LSCC in a live medium are insufficient [2, 3]. Therefore, we suggest establishing chick embryo chorioallantoic membrane (CAM) assay for this type of tumor as a medium that reveals numerous unique properties and advantages [4, 5].

Because the chick embryo CAM model has been used for scientific purposes for decades, the system is quite well described in the literature and some evident benefits of the CAM assay are emphasized [6, 7]. The immatureness of the chick embryo immune system allows using different cell types and cells from different tissues and species. Consequently,

the chick embryo CAM assay is considered as simple, rapid, and cost effective, if compared with most *in vivo* models [4].

Therefore, we propose that the chick embryo CAM model can be successfully used to characterize LSCC morphology, invasion, angiogenic response *in vivo*, and metastatic properties. Remarkable proof is the evidence that the chick embryo CAM model has substantially contributed to several Nobel Prize laureates' scientific discoveries including the first known oncogene [8], neural growth factor based on effects of mouse tumor transplantation [9], and the interaction between tumor viruses and the genetic material of the cell [10].

The chick embryo develops 21 days until hatching out. The CAM is formed on days 4 to 5 of incubation as a consequence of fusion of mesodermal layers of outgrowing allantois and the chorion. The newly formed membrane is composed of chorionic and endodermal epithelia with an intricate plexus of arteries, veins, and capillaries. The highly vascularized nature of this assay is a considerable advantage which greatly stimulates the growth of the xenogeneic tumor and facilitates the analysis of angiogenic effect of implanted tumor on the CAM [11]. This feature determines the use of the CAM as a perfect medium for tumor implanting, studying carcinoma behavior and development. It is probably the most widely used *in vivo* assay for studying angiogenesis [4, 11, 12].

One of the greatest features of chick embryo CAM assay is an incomplete lymphoid system which is not fully developed until the late stages of incubation. The chick embryo may serve as a naturally immunodeficient host that is efficient for maintaining implanted tumor tissues without species-specific restrictions [11]. It is known that after the chick embryo becomes immunocompetent (the 18th day of incubation), both acute and chronic inflammatory responses of the CAM to biomaterials become similar to those of mammalian ones [4]. Data of the literature show that chick genes have a single human orthologue with an accuracy of about 60%. Chick and human orthologous genes reveal lower sequence conservation (75.3%) than rodent and human do (88%) [4]. Therefore, the avian model can be used for research in more fields of investigation compared to rodent ones. Moreover, no special permission from the Animal Rights Protection Committee is needed to perform the experimentation with chick embryo in both the European Union and USA. A great support to perform this type of investigation is approbation obtained from the US Food and Drug Administration and the Communication Department of the European Commission (2006) for the products that are preclinically evaluated using this assay [4].

Most of the avian experimental models such as human osteosarcoma, human colon carcinoma, and others used cells from the tumor cell lines implanted in the chick embryo CAM [11, 13, 14]. However, it can be presumed that this type of experiment while implanting cultivated tumor cells loses most of the natural physiological and histological features of the original tumor. Several *in vitro* models have been developed in the last few decades to investigate the oncogenic phenotypes of different malignant tumors. However, most of these models employed monolayer cell cultures, making these assays difficult to translate to clinical applications [6].

Following the experience obtained from glioblastoma tumor implantation on the chick embryo CAM [15], we suggested implanting fresh laryngeal tumor samples onto the chick embryo CAM [16], expecting that the tumor will retain its physiological properties and will show analogous behavior as in its natural environment. We demonstrated that fresh LSCC tissue samples remain viable with their main histological features up to 4 days after implantation onto the chick embryo CAM.

The aim of this study was to evaluate the morphological and morphometric characteristics and angiogenic features of the chick embryo CAM LSCC model. In this study, we used the chick embryo CAM for the first time to investigate the angiogenic effect of LSCC and to provide the morphometric characteristics of the CAM LSCC model. The implanted tumor induced considerable morphological changes of the CAM structures and demonstrated significant instigated vascularization of the host membrane.

2. Materials and Methods

2.1. Incubation and Egg Opening. Fertilized hen eggs (*Cobb-500*) were obtained from the local hatchery (Dovainonių Paukštynas, Lithuania) and were incubated at 37.7°C temperature and 59-60% relative humidity with permanent ventilation and rotation. On the third embryonic day (approximately 72 hours of incubation) eggs' shells were sterilized with 70% ethanol solution. The blunt part of the egg was punctured searching for the air chamber. Two milliliters of albumen was removed in order to set down the developing embryo. Then, an oval window of about 1.0 cm^2 on the top of the shell of each egg was opened using a high speed drill. All embryos were examined for possible malformations or signs of local bleeding. Those embryos that did not satisfy the study requirements were discarded.

In order to prevent embryos from dehydration and to capacitate the continuity of the experiment the shell windows were covered with transparent sterile tape. After this procedure, the prepared eggs were placed back into the incubator and kept under the same conditions without rotation for 4 to 6 days until implantation of the LSCC tissue.

2.2. LSCC Tissue Samples. Fresh LSCC tissue samples ($N = 6$) of at least about $0.5 \times 1.0 \times 0.5$ cm in size were obtained from 6 patients at the Department of Otorhinolaryngology during laryngeal surgery. Diagnosis of the LSCC was proved at the Department of Pathology. The LSCC tissue samples were transported to the laboratory of the Department of Histology and Embryology in isotonic saline solution at ambient temperature (18–20°C) and then implanted onto the chick embryo CAM within 45–60 minutes.

Investigations in the present study were performed in accordance with the principles outlined in the Declaration of Helsinki and approved by Kaunas Regional Bioethics Committee (P1-BE-2-34/2007). Histologically confirmed LSCC tissue samples were acquired in accordance with the protocol approved by the Institutional Review Board of LUHS. Written Informed Consent was obtained from the patients before

surgery and patients' identifiers were removed to ensure anonymity.

2.3. LSCC Tissue Implantation onto the CAM. LSCC implantation was performed on the 7th, 8th, or 9th day of eggs' incubation when the CAM is already formed. Each LSCC tissue sample obtained directly from the operating room was sliced into approximately 8 mm^3 pieces. Each piece of the tumor (1 piece per egg) was gently placed on the outer surface of the CAM near the biggest apparent vessel of the membrane, that is, using classical technique as it is described by Cushman et al. [17]. On the 11th day of eggs' incubation, that is, after 48, 72, and 96 hours of tumor implantation, two eggs were reopened and live-fixed in the 10% formalin solution. CAMs with the adhering tumors were excised and fixed in formalin for 5 days. Eight control CAMs were obtained on the 11th day from eggs that were incubated and proceeded under the same protocol, except the LSCC tissue implantation.

2.4. Tissue Sampling and Histology. Formalin-fixed and paraffin-embedded samples of approximately 0.5×2.5 cm in size from each CAM with LSCC implant were sliced into 3 μm thick sections and stained with hematoxylin and eosin (H&E) for histological and morphometric evaluation. Histological evaluation of the samples was performed with the cold light microscope OLYMPUS BX40F4 (Olympus Optical Co. Ltd., Japan) under 10x magnification using CellSens Dimension 1.9 Digital Imaging Software for Research Applications (Olympus Corporation of the Americas, USA).

2.5. Immunohistochemistry. For immunohistochemical examination, the 3 μm thick slices of paraffin-embedded CAMs with LSCC implants as well as original tumor tissue slices were mounted on poly-L-lysine coated glass slides. After deparaffinization with xylene and rehydration the sections were pretreated with antigen-retrieval solution (0.01 mol/L of citrate buffer, pH 6) in a pressure-cooker and then incubated: (1) with cytokeratin monoclonal antibodies (clone 34βE12, dilution 1 : 50) for identification of high molecular weight cytokeratin (HMW CK), because previous studies have shown squamous cell carcinomas being positive for these antibodies [18], (2) with monoclonal mouse anti-human CD31 (endothelial cell clone JC70A, dilution 1 : 40) for detection of vascular endothelial cells in tumor tissue [19, 20], and (3) with monoclonal mouse anti-human antibody for Ki67 (clone MIB-1, dilution 1 : 50) to identify nuclei of proliferating tumor cells [21].

All antibodies were purchased from Dako A/S (Glostrup, Denmark). Antibodies' detection using commercially available kit EnVision Plus-HRP, Dako A/S, was performed following the protocols of the provider. Sections were counterstained in weak Mayer's hematoxylin, dehydrated, cleared, and mounted for the light microscopy.

2.6. Histochemistry of Mesodermal CAM Vessels. For visualization of CAM blood vessels, paraffin-embedded tissue samples were sliced in 3 μm thick slices and mounted on poly-L-lysine coated glass slides. Sections were rehydrated as previously described and pretreated with streptavidin/biotin blocking kit (Vector, USA). In order to highlight endothelium of blood vessels in chick embryo CAM, slices were stained with 10 μg/mL biotinylated *Sambucus nigra* bark lectin (Vector, USA) [22]. The VECTASTAIN *Elite ABC* kit was used (Vector, USA) to detect biotinylated molecules. Enzyme activity sites were visualized using DAB chromogen solution (Dako, Denmark). Sections were counterstained in Mayer's hematoxylin, dehydrated, cleared, and mounted. *Sambucus nigra* lectin specifically binds to chick endothelium; therefore, the blood vessels were seen brown under the light microscope (Figures 1(c) and 1(d)).

2.7. Histomorphometric Analysis. Histomorphometric evaluation of the CAM parameters was performed on the images obtained with Olympus digital camera (Olympus U-CMAD3, Philippines). To perform accurate morphometric analysis each CAM section was divided into 5 sight fields (SFs) (Figure 1(a)). The central location directly under the implanted tumor was defined as the first SF, the 2nd and 4th SFs were defined as neighboring sites, and the 3rd and 5th SFs were defined as distant SFs, respectively. The thicknesses of both the CAM and the chorionic epithelium were measured in all SFs. The parameters measured only in central and neighboring SFs (the 1st, 2nd, and 4th) were as follows: (1) number of blood vessels with the smallest diameter of not less than 8 μm per constant length of the CAM section and (2) mean area of the counted blood vessels' cross-section. The latter were identified following the endothelial cells and erythrocytes inside the lumen of blood vessels in *Sambucus nigra* lectin (Figures 1(c) and 1(d)) and H&E stained sections, according to the systematic sampling approach of Russ and Dehoff [23]. Eight control CAMs were processed under the same conditions, except that measurements of each parameter were performed in five random SFs (Figures 1(b)–1(d)).

2.8. Statistical Analysis. Statistical analysis was performed using IBM SPSS Statistics for Windows, Version 20.0 (Armonk, NY: IBM Corporation Software). Data were presented as the mean ± standard deviation (SD). Student's t-test was used to test hypothesis with respect to equality of means. The size of the differences among the mean values of the groups was evaluated by estimation of type I and type II errors (α and β) of the tests. The difference was considered to be significant if $\beta \leq 0.2$ and $\alpha = 0.05$. The correlations among the number of blood vessels and the thickness of the CAM and the thickness of epithelium of the CAM were evaluated using Pearson's correlation coefficient (r). The level of statistical significance for testing statistical hypothesis was 0.05.

3. Results

The laryngeal squamous cell carcinoma tissue samples ($N = 6$) were tested on chick embryo CAMs ($N = 120$). In this paper we evaluate the effect of LSCC for those CAMs that were cut off on the 11th incubation day, that is, 2, 3, and 4 days after tumor tissue implantation ($N = 15$). All 15 CAMs

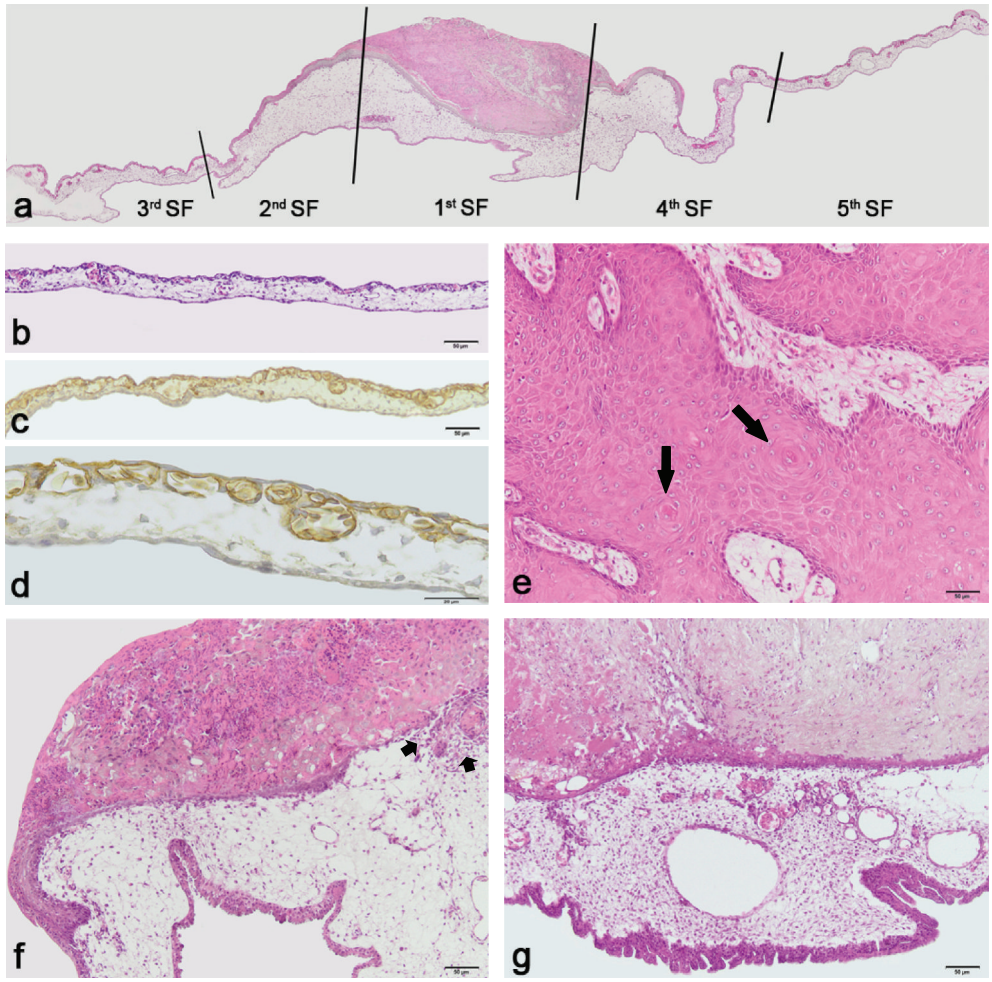

Figure 1: Histological appearance of the control and experimental CAM and LSCC tissue. (a) Sight fields of CAM with LSCC implant; original magnification 4x. (b–d) The control CAMs: stained in H&E (b); CAM's blood vessels revealed with *Sambucus nigra* lectin (c, d). (e) Moderately differentiated squamous cell carcinoma of the larynx. Accumulation of atypical cells with concentrically arranged keratinized cells ("carcinoma pearls": long arrows) was observed in the original LSCC tissue. (f) Thickened CAM and chorionic epithelium of experimental group with LSCC implant: invasion through epithelium (short arrows). (g) Increased vascularity under the LSCC implant. (b, c, e, f, and g) Bars 50 μm; original magnification 10x; (d) bar 20 μm; original magnification 40x.

were evaluated morphologically in numerous sections and morphometric parameters were obtained in 5 SFs of 4 nonserial sections (Figure 1(a)). Three hundred SFs were measured accordingly.

CAMs ($N = 8$) without implants served as controls. Measurements of control CAMs were made in 160 SFs using the same methods (Figures 1(b)–1(d)).

The original LSCC tissue was evaluated histologically. Typical signs of the tumor were observed: the parenchyma consisted of atypical epithelial cells with irregular nuclei and increased number of nucleoli. Accumulation of atypical cells with concentrically arranged keratinized cells ("carcinoma pearls") was observed (Figure 1(e)). The surrounding stroma was composed of loose connective tissue showing different level of infiltration by monomorphonuclear cells.

3.1. Histological and Immunohistochemical Characteristics of Implanted LSCC Tissue. The implanted LSCC tissue samples consisted of solid pieces of polymorphous atypical squamous epithelial cells with large irregular nuclei and increased mitosis, while observing one or several prominent nucleoli and abundant acidophilic cytoplasm. The tumor cells retained their vitality in 2, 3, and 4 days after implantation and the apparent influence of the LSCC on the CAM was observed (Figures 1(f) and 1(g)). The implanted tumor tissues on the chick embryo CAM in all the cases were visibly adhered to the host CAM and never flowed away.

The HMW CK (CK34βE12) was expressed in the cytoplasm of the original LSCC epithelial cells. Epithelial cells of the LSCC implanted on the CAM also showed high positivity for the HMW CK. Endothelial cells of the blood vessels were positive for CD31 in both the original and implanted LSCC tissues. Cellular marker for proliferation Ki67 was positive in the nuclei of the original tumor cells (Figures 2(a) and 2(c)) also showing positivity for HMW CK (Figure 2(b)). Expression of CD31 in implanted LSCC blood

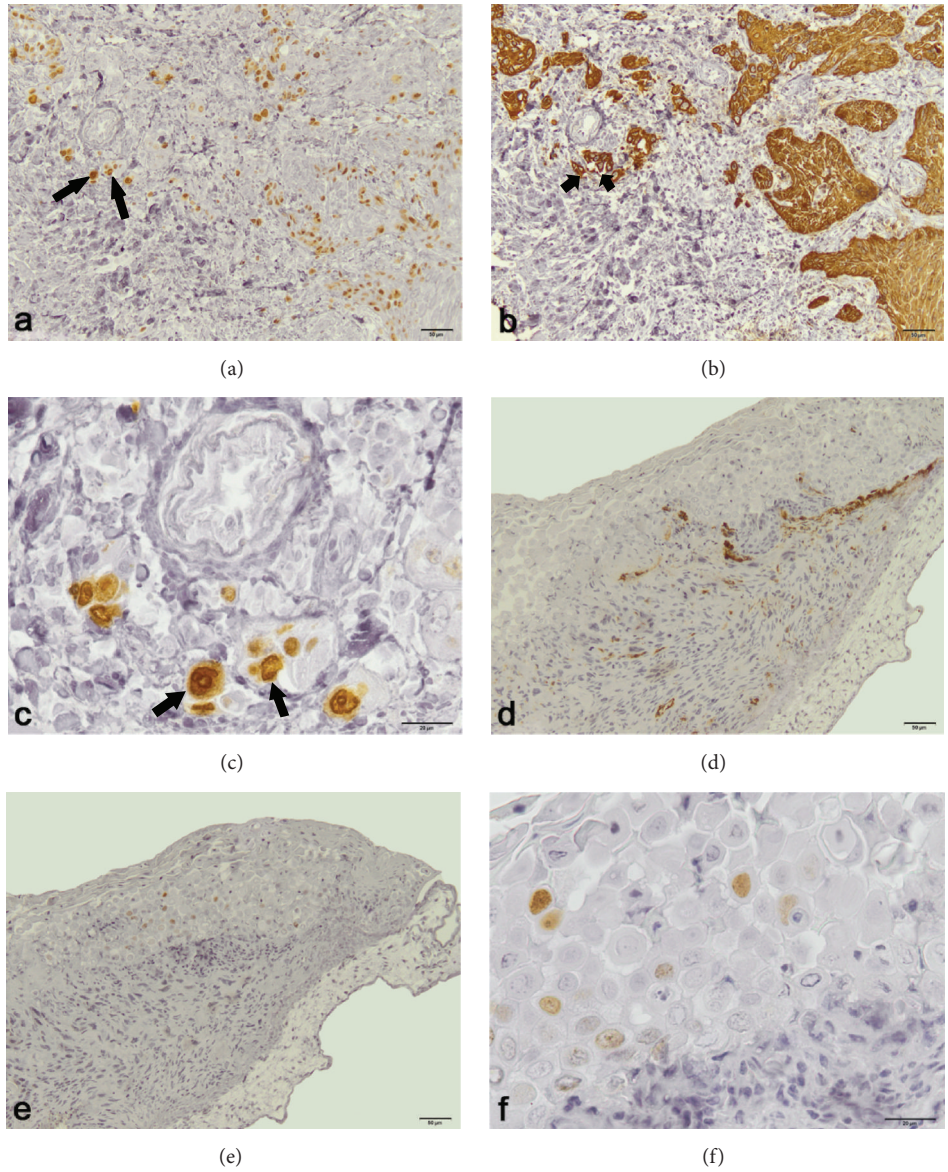

Figure 2: An immunohistochemical study of LSCC tissue before and after implantation on CAM. (a, c) The original tumor cells, which showed high positivity for the Ki67 (long arrows). (b) The original tumor cells (the same site as in (a)) were also positive for HMW CK (short arrows). (d) Endothelial cells of implanted tumor blood vessels were positive for CD31. (e, f) Ki67 positive nuclei of implanted LSCC cells. (a, b, d, and e) Bars 50 μm; original magnification 10x; (c, f) bars 20 μm; original magnification 40x.

vessels (Figure 2(d)) and Ki67 in its epithelial cells (Figures 2(e) and 2(f)) indicated that the implanted tissue retained features of the original tumor and preserved proliferative capacity even after 96 hours after the implantation.

3.2. Morphometric and Morphologic Characteristics of the CAM. The morphological features of the CAMs' reaction induced by the LSCC implants were similar in all specimens of the experimental group. Thus, there were no significant differences between morphological features of the different CAMs with implants obtained from the same patient as well. Results of the morphometric analysis of the CAMs in experimental and control groups are presented in Table 1. The mean thickness of the CAM under the implanted LSCC in the experimental group was statistically significantly ($p = 0.0001$) increased in all 5 SFs comparing to that of the control group. The largest difference between the thickness of the experimental and the control CAMs was found in the central SF (1st SF) and reached 417%. However, in the distant SFs (3rd and 5th SFs) the difference was less and reached 103–109%, respectively. Furthermore, in the experimental group the host CAM in the central SF was statistically significantly thicker than in the neighboring and the distant SFs, respectively ($p < 0.05$).

Table 2 shows the mean thickness of the CAMs in both experimental and control groups 2, 3, and 4 days after

Table 1: Mean thickness of the CAM: experimental group versus control group.

	LSCC group		Control group		Difference			
Sight fields	Mean μm	SD	Mean μm	SD	μm	%	p	β
1st SF	204.9	143.9	37.1	16.4	167.9	417	0.0001	<0.01*
2nd SF	132.7	101.6			95.6	235	0.0001	<0.01*
3rd SF	83.0	71.5			45.9	109	0.0001	<0.01*
4th SF	124.7	98.9			87.7	214	0.0001	<0.01*
5th SF	80.7	79.3			43.7	103	0.0001	<0.01*

*Statistically significant difference between the groups, computed using $\alpha = 0.05$.

Table 2: Mean thickness of the CAM 2, 3, and 4 days after the LSCC tumor implanting: experimental group versus control group.

	LSCC group		Control group		Difference			
Days after LSCC implantation	Mean μm	SD	Mean μm	SD	μm	%	p	β
2nd day	102.8	97.1	37.1	16.4	66.8	177	0.001	<0.01*
3rd day	104.9	52.8			67.9	183	0.001	<0.01*
4th day	185.8	137.6			148.7	401	0.001	<0.01*

*Statistically significant difference between the groups, computed using $\alpha = 0.05$.

the LSCC tumor implantation (i.e., totally 11 days of incubation). The mean thickness of the CAM was statistically significantly higher ($p = 0.001$) in the experimental group versus control group already 2 days after the tumor implantation reaching 177%. Of note, on the 4th day after the LSCC tumor implantation that difference reached 401%. There was no positivity for the HMW CK in the mesenchymal layer or endodermal epithelium of the CAM. Expression of CD31 and Ki67 was not detected in the CAM as well.

3.3. Morphometric and Morphologic Characteristics of the CAM Epithelium. The chorionic epithelium in the experimental group was found to be thickened in comparison with the control group (Table 3) and it appeared squamous and stratified, consisting of 5-6 layers. The mean thickness of the epithelium under the LSCC implant was statistically significantly ($p = 0.0001$) higher as compared with the control group. The highest difference was found in the 1st SF (140%) while in the distant SFs these differences reached 70 and 75%, respectively.

All implanted tumors induced similar morphometric characteristics of the CAM epithelium under the LSCC implants. No significant differences were found in the morphometric characteristics of the epithelium after implanting the same patient's tumor on different CAMs ($p > 0.05$). However, there were certain regions of the CAM under the LSCC implants with thinned and even discontinuous epithelium (Figure 1(f)) and signs of tumor cells' invasion. Adjacent mesenchyme showed a dense accumulation of blood vessels immediately below the implant (Figure 1(g)).

The keratogenic metaplasia in the chorionic epithelium just beneath the implanted LSCC was detected by positive immunostaining with HMW CK. However, keratogenic metaplasia has never been found in the distant SFs of the experimental CAMs, as well as in the CAM epithelium of the control group.

3.4. Histomorphological Characteristics of the Vascularity of the CAM. Histomorphometric evaluation revealed a statistically significant difference of the mean number of CAM blood vessels between the experimental and control groups ($p = 0.0001$) (Table 4). The experimental group had much higher mean number of blood vessels per constant length of the CAM, thus demonstrating measurable evidence of increased vascularity. The highest difference from the control CAM was in the 1st SF reaching 148%; however, in neighboring SFs the difference was less: 92% and 75%, respectively.

The mean number of blood vessels under the LSCC tissue implant (the 1st SF) was found to be significantly higher in comparison with the neighboring sites ($p < 0.05$) of the experimental CAM.

The statistically significant ($p < 0.05$) moderate positive correlations between the number of blood vessels and the thickness of the CAM ($r = 0.65$), as well as the thickness of epithelium of the CAM ($r = 0.37$), were revealed in the experimental group.

As shown in Table 5, the mean area of blood vessels' lumen in the experimental group was statistically significantly larger in all SFs if compared with that of the control group. In the 1st SF the difference between the experimental and control groups reached 155%, in the neighboring SFs, 106% and 82%, respectively.

4. Discussion

The chick embryo CAM model has long been used for the investigation of angiogenesis, oncogenesis, and tumor metastasis [24–26]. This model provides a naturally immunodeficient host that accepts implantation from various tissues

Table 3: Mean thickness of the CAM epithelium: experimental group versus control group.

	LSCC group		Control group		Difference			
Sight fields	Mean μm	SD	Mean μm	SD	μm	%	p	β
1st SF	14.9	5.6	6.22	1.2	8.7	140	0.0001	<0.01*
2nd SF	12.9	7.2			6.78	107	0.0001	<0.01*
3rd SF	10.9	5.5			4.7	75	0.0001	<0.01*
4th SF	11.9	4.7			5.7	91	0.0001	<0.01*
5th SF	10.6	6.2			4.5	70	0.0001	<0.01*

*Statistically significant difference between the groups, computed using $\alpha = 0.05$.

Table 4: Mean number of blood vessels per constant length of the CAM section: experimental group versus control group.

	LSCC group		Control group		Difference			
Sight fields	Mean	SD	Mean	SD	Absolute	%	p	β
1st SF	15.9	10.8	6.4	2.9	9.5	148	0.0001	<0.01*
2nd SF	12.3	5.5			5.9	92	0.0001	<0.01*
4th SF	11.2	5.8			4.9	75	0.0001	<0.01*

*Statistically significant difference between the groups, computed using $\alpha = 0.05$.

Table 5: Mean area of the CAM blood vessel lumen: experimental group versus control group.

	LSCC group		Control group		Difference			
Sight fields	Mean μm^2	SD	Mean μm^2	SD	μm^2	%	p	β
1st SF	169.3	119.5	66.4	42.8	102.9	155	0.0001	<0.01*
2nd SF	138.9	127.9			72.4	109	0.0001	<0.01*
4th SF	121.0	79.7			54.6	82	0.0001	<0.05*

*Statistically significant difference between the groups, computed using $\alpha = 0.05$.

and species and therefore can be used for xenoimplantation of different types of cells. The extraembryonic membranes that are connected to the embryo through a continuous extraembryonic vessel system are readily accessible for experimental manipulation and observations [27]. Despite the evident advantages of the CAM assay and its natural immunodeficient environment, the chick embryo CAM model is still relatively rarely used for implanting of human tumors. Nevertheless, there are several reports about the employment of the CAM assay as a reliable model to study various human tumors, namely, melanoma [28], prostatic cancer [29], glioblastoma [15, 30], human colon carcinoma [13], giant cell tumor of bone [14], sarcoma [31], and head and neck squamous cell carcinoma [6].

However, there are only sporadic reports in the literature about the use of the CAM assay for biological studies of human laryngeal tissue: for establishment of LSCC cell lines [2] and for CAM analysis of cellular laryngeal scaffolds showing induction of a strong *in vivo* angiogenic response [24].

On the other hand, most experiments with chick embryo CAM reported in the literature used tumor cell lines that did not represent the natural physiological features of a solid tumor. Experiments with cell lines might not fully reflect the wide heterogeneity of human malignancies, because of poor correlation between the behavior of single cell lines *in vitro* and tumors encountered in patients. Depurated cancer cell lines differ genetically from the original cancers in patients, because these cells have a phenotype adapted to culturing on plastic substrates that are commonly employed in xenograft experiments [31]. Positive performance of an exploratory drug in experimental xenografts of different human cancer cell lines is not predictive enough of compound efficacy in the clinical setting [32].

The use of fresh tumor samples for the CAM assay preserves the original tumor microenvironment of the heterogeneous tumor cell population and the associated matrix allowing natural interactions between the different cell populations in the sample [31]. Therefore, preservation of the microenvironment is a theoretical benefit of using fresh tumor samples.

The results of our study indicate that LSCC tissue samples outlived on the CAMs sustaining strongly adhered to the membranes in all the experiments despite the short term of interaction (2 to 4 days after implantation). All examined implants retained essential characteristics of the donor tumor specimens from living individuals with LSCC. It is important to note that all LSCC implants remained with their main histological features and no signs of necrosis were observed. Thus, the results of the present study show that the CAM assay

can be used to analyze fresh material derived from LSCC. This is the first *in vivo* model for LSCC which opens new perspectives to study this disease and tumor aggressiveness and to assess tumor responses to new therapeutic agents.

We have noticed that LSCC tissues induced significant changes of all the structures of the host medium starting from the 2nd day after tumor implantation while having stayed on the CAM. The observed thickening of the mesenchyme with increased density of mesenchymal cells and thickening of chorionic epithelium in the CAM under the tumor implant can be explained as the result of action of the growth stimuli factors that are coming from the implanted LSCC tumor tissue and the nonspecific inflammatory reaction of the CAM due to the implant [33, 34].

Examination of CAM sections suggested that partial thickening in the mesenchyme between the outer and inner epithelium may be due to edema [35]. During the investigation with the uncoated dialysis capillary or by applying the Thermanox tissue culture cover slips onto the CAM, a high density of inflammatory cells, such as heterophils, and giant mast cells with associated fibrosis were found. The stroma of the CAM showed fibrocyte proliferation, leucocyte infiltration, and clusters of dispersed ectodermal epithelial cells [36–39]. As chick embryo CAM is accepted to be a naturally immunodeficient host [11] until day 18 of incubation [4], the inflammatory response of the chorioallantoic membrane to biomaterials is explained as the result of appearance of nonlymphoid avian leukocytes, mast cells, basophils, thrombocytes (functional analog to platelets), and monocytes that represent nonspecific inflammatory reaction [33].

Angiogenesis plays a critical role in many normal physiological processes, as well as in tumor neovascularization [34]. Establishment and growth of malignant tumors are critically dependent on their ability to stimulate the formation of new blood vessels from preexisting vasculature to support their metabolic needs [34, 40]. Thus, angiogenesis facilitates tumor growth and spread [6].

In head and neck tumors, increased angiogenesis has been associated with an unfavorable prognosis in many studies; however, prognostic relevance of angiogenic factors in laryngeal tumor development has been questioned [41–43]. More recent studies emphasized that increased LSCC tumor angiogenesis was an early event in laryngeal tumor development and positively correlated with local and locoregional relapse and lethal outcome of the disease [44, 45].

Chick embryo CAM being rich in developed arteries, veins, and capillary plexus also accompanied by evolved nutrition delivery system is accepted to be one of the most widely used *in vivo* assays for studying anti- or proangiogenic properties [4, 12, 34]. However, theoretically, revascularization of the tumor sample is required for the sample's survival and growth [31].

The results of our study disclose that after implanting fresh LSCC tissue samples onto the chick embryo CAM the process of active angiogenesis in the CAM appears. That is the result of multiplying blood vessels associated with increase in vessel volume; hence, nascent blood vessel proliferation during our experiment is the visible sign of LSCC progression onto the CAM.

It is suggested though that alteration in the gaseous environment of chorionic epithelium may have initiated the chain of events leading to keratogenic metaplasia [46]. This phenomenon has been noticed while investigating LSCC implant onto chick embryo CAM in our study: the keratogenic metaplasia in the chorionic epithelium was observed only just beneath the implanted LSCC in contrast to the sites distant from the carcinoma implant or CAMs of control.

Results of the present study are in agreement with the data of other investigations. An increased value of vascular growth was noticed after implantation of decellularized healthy laryngeal tissue samples on CAM [24]. Ovarian fragments implanted onto chick embryo CAM markedly increased the number of distended blood vessels in the membrane near or next to the implanted ovarian fragments and an increased number of fine capillaries within close proximity of the implanted fragments were found [17, 27]. The gastrointestinal tract carcinoma cells induced angiogenesis in the CAM and positively correlated with their capacity to colonize the CAM tissue [13, 25].

The results of our study show that reliable protocol for implanting of human LSCC onto the chick embryo CAM is established and this assay can be used to analyze fresh material derived from human LSCC. However, some limitations arise from the inherent features of the chick embryo CAM model. Because the duration of the CAM assay is limited to a 7–9 days' window available before the chick hatches, most tumor cells cannot produce macroscopically visible colonies in secondary organs before the termination of the assay. As a result, the more difficult detection of micrometastases becomes an inherent part of the chick embryo CAM model system [47]. This feature of the chick embryo CAM assay probably determined a rather rare (2 cases out of 6) detection of LSCC invasion and micrometastases in our series.

5. Conclusions

In summary, results of our study clarify that chicken embryo CAM is a relevant host medium for implanting fresh tissues of the LSCC. The LSCC implants adhere to the host membrane and induce significant morphological changes of it, allowing visualizing microscopically the behavior of implanted tumor cells. Data of this study provide the first morphological and morphometric characterization of the LSCC implant on CAM model and, therefore, allow better understanding of cancer cell biology. Future development of this model may lead to identification of new specific and selective therapeutic agents and composition of drugs to limit spread of LSCC.

Abbreviations

LSCC: Laryngeal squamous cell carcinoma
CAM: Chorioallantoic membrane
SD: Standard deviation
SF: Sight field
HMW CK: High molecular weight cytokeratins.

Conflict of Interests

The authors declare that they have no conflict of interests.

Acknowledgments

The authors highly appreciate the technical assistance of Valda Saročkaitė and Raminta Mozūraitė from Department of Histology and Embryology, LUHS.

References

[1] E. Rudolph, G. Dyckhoff, H. Becher, A. Dietz, and H. Ramroth, "Effects of tumour stage, comorbidity and therapy on survival of laryngeal cancer patients: a systematic review and a meta-analysis," *European Archives of Oto-Rhino-Laryngology*, vol. 268, no. 2, pp. 165–179, 2011.

[2] D. M. Easty, G. C. Easty, A. Baici et al., "Biological studies of ten human squamous carcinoma cell lines: an overview," *European Journal of Cancer and Clinical Oncology*, vol. 22, no. 6, pp. 617–634, 1986.

[3] D. Sano and J. N. Myers, "Xenograft models of head and neck cancers," *Head & Neck Oncology*, vol. 1, article 32, 2009.

[4] A. Vargas, M. Zeisser-Labouèbe, N. Lange, R. Gurny, and F. Delie, "The chick embryo and its chorioallantoic membrane (CAM) for the in vivo evaluation of drug delivery systems," *Advanced Drug Delivery Reviews*, vol. 59, no. 11, pp. 1162–1176, 2007.

[5] D. Ribatti, "The chick embryo chorioallantoic membrane as a model for tumor biology," *Experimental Cell Research*, vol. 328, no. 2, pp. 314–324, 2014.

[6] M. Liu, C. S. Scanlon, R. Banerjee et al., "The histone methyltransferase EZH2 mediates tumor progression on the chick chorioallantoic membrane assay, a novel model of head and neck squamous cell carcinoma," *Translational Oncology*, vol. 6, no. 3, pp. 273–281, 2013.

[7] D. Ribatti, "The chick embryo chorioallantoic membrane as an in vivo assay to study antiangiogenesis," *Pharmaceuticals*, vol. 3, no. 3, pp. 482–513, 2010.

[8] D. Stehelin, H. E. Varmus, J. M. Bishop, and P. K. Vogt, "DNA related to the transforming gene (s) of avian sarcoma viruses is present in normal avian DNA," *Nature*, vol. 260, no. 5547, pp. 170–173, 1976.

[9] M. N. Vergara and M. V. Canto-Soler, "Rediscovering the chick embryo as a model to study retinal development," *Neural Development*, vol. 7, no. 1, article 22, 2012.

[10] H. M. Temin, "The participation of DNA in Rofs sarcoma virus production," *Virology*, vol. 23, no. 4, pp. 486–494, 1964.

[11] E. I. Deryugina and J. P. Quigley, "Chick embryo chorioallantoic membrane model systems to study and visualize human tumor cell metastasis," *Histochemistry and Cell Biology*, vol. 130, no. 6, pp. 1119–1130, 2008.

[12] C. A. Staton, S. M. Stribbling, S. Tazzyman, R. Hughes, N. J. Brown, and C. E. Lewis, "Current methods for assaying angiogenesis *in vitro* and *in vivo*," *International Journal of Experimental Pathology*, vol. 85, no. 5, pp. 233–248, 2004.

[13] M. C. Subauste, T. A. Kupriyanova, E. M. Conn, V. C. Ardi, J. P. Quigley, and E. I. Deryugina, "Evaluation of metastatic and angiogenic potentials of human colon carcinoma cells in chick embryo model systems," *Clinical and Experimental Metastasis*, vol. 26, no. 8, pp. 1033–1047, 2009.

[14] M. Balke, A. Neumann, C. Kersting et al., "Morphologic characterization of osteosarcoma growth on the chick chorioallantoic membrane," *BMC Research Notes*, vol. 3, article 58, 2010.

[15] N. Balčiuniene, A. Tamašauskas, A. Valančiute et al., "Histology of human glioblastoma transplanted on chicken chorioallantoic membrane," *Medicina*, vol. 45, no. 2, pp. 123–131, 2009.

[16] A. Kuzminienė, S. Šalomskaitė-Davalgienė, I. Balnyte, J. Palubinskienė, A. Valančiūtė, and V. Ulozas, "Evaluation of the chicken embryo chorioallantoic membrane model for laryngeal tumor transplantation," *Papers on Anthropology*, vol. 20, pp. 229–240, 2012.

[17] R. A. Cushman, C. M. Wahl, and J. E. Fortune, "Bovine ovarian cortical pieces grafted to chick embryonic membranes: a model for studies on the activation of primordial follicles," *Human Reproduction*, vol. 17, no. 1, pp. 48–54, 2002.

[18] M. Scarpatetti, O. Tsybrovskyy, and H. H. Popper, "Cytokeratin typing as an aid in the differential diagnosis of primary versus metastatic lung carcinomas, and comparison with normal lung," *Virchows Archiv*, vol. 440, no. 1, pp. 70–76, 2002.

[19] D. Wang, C. R. Stockard, L. Harkins et al., "Immunohistochemistry in the evaluation of neovascularization in tumor xenografts," *Biotechnic and Histochemistry*, vol. 83, no. 3-4, pp. 179–189, 2008.

[20] A. B. Villaret, D. Barbieri, G. Peretti et al., "Angiogenesis and lymphangiogenesis in early-stage laryngeal carcinoma: prognostic implications," *Head and Neck*, vol. 35, no. 8, pp. 1132–1137, 2013.

[21] R. B. Rodrigues, R. Da Ros Motta, S. M. Dos Santos Machado et al., "Prognostic value of the immunohistochemistry correlation of Ki-67 and p53 in squamous cell carcinomas of the larynx," *Brazilian Journal of Otorhinolaryngology*, vol. 74, no. 6, pp. 855–859, 2008.

[22] M. Brand, N. Lamandé, E. Larger, P. Corvol, and J.-M. Gasc, "Angiotensinogen impairs angiogenesis in the chick chorioallantoic membrane," *Journal of Molecular Medicine*, vol. 85, no. 5, pp. 451–460, 2007.

[23] J. C. Russ and R. T. Dehoff, *Practical Stereology*, Plenum Press, New York, NY, USA, 2nd edition, 1999.

[24] S. Baiguera, A. Gonfiotti, M. Jaus et al., "Development of bioengineered human larynx," *Biomaterials*, vol. 32, no. 19, pp. 4433–4442, 2011.

[25] D. I. Gheonea, T. Cârtâna, T. Ciurea, C. Popescu, A. Badarau, and A. Saftoiu, "Confocal laser endomicroscopy and immunoendoscopy for real-time assessment of vascularization in gastrointestinal malignancies," *World Journal of Gastroenterology*, vol. 17, pp. 21–27, 2011.

[26] D. Ribatti, *The Chick Embryo Chorioallantoic Membrane in the Study of Angiogenesis and Metastasis*, Springer Science+Business Media B.V, London, UK, 2010.

[27] V. Isachenko, P. Mallmann, A. M. Petrunkina et al., "Comparison of in vitro- and chorioallantoic membrane (CAM)-culture systems for cryopreserved medulla-contained human ovarian tissue," *PLoS ONE*, vol. 7, no. 3, Article ID e32549, 2012.

[28] I. C. MacDonald, E. E. Schmidt, V. L. Morris, A. F. Chambers, and A. C. Groom, "Intravital videomicroscopy of the chorioallantoic microcirculation: a model system for studying metastasis," *Microvascular Research*, vol. 44, no. 2, pp. 185–199, 1992.

[29] K. Kunzi-Rapp, F. Genze, R. Küfer, E. Reich, R. E. Hautmann, and J. E. Gschwend, "Chorioallantoic membrane assay: vascularized 3-dimensional cell culture system for human prostate

cancer cells as an animal substitute model," *Journal of Urology*, vol. 166, no. 4, pp. 1502–1507, 2001.

[30] M. Hagedorn, S. Javerzat, D. Gilges et al., "Accessing key steps of human tumor progression in vivo by using an avian embryo model," *Proceedings of the National Academy of Sciences of the United States of America*, vol. 102, no. 5, pp. 1643–1648, 2005.

[31] G. Sys, M. Van Bockstal, R. Forsyth et al., "Tumor grafts derived from sarcoma patients retain tumor morphology, viability, and invasion potential and indicate disease outcomes in the chick chorioallantoic membrane model," *Cancer Letters*, vol. 326, no. 1, pp. 69–78, 2012.

[32] J. S. De Bono and A. Ashworth, "Translating cancer research into targeted therapeutics," *Nature*, vol. 467, no. 7315, pp. 543–549, 2010.

[33] T. I. Valdes, D. Kreutzer, and F. Moussy, "The chick chorioallantoic membrane as a novel *in vivo* model for the testing of biomaterials," *Journal of Biomedical Materials Research*, vol. 62, no. 2, pp. 273–282, 2002.

[34] E. I. Deryugina and J. P. Quigley, "Chapter 2 chick embryo chorioallantoic membrane models to quantify angiogenesis induced by inflammatory and tumor cells or purified effector molecules," in *Methods in Enzymology*, vol. 444, pp. 21–41, Elsevier, 2008.

[35] British American Tobacco, *Research & Development Establishment: Report No. RD. 680: A Chorioallantoic Membrane Hyperplasia Test for Smoke*, British American Tobacco, Southampton, UK, 1969.

[36] G. J. Burton and M. E. Palmer, "Development of the chick chorioallantoic capillary plexus under normoxic and normobaric hypoxic and hyperoxic conditions: a morphometric study," *Journal of Experimental Zoology*, vol. 262, no. 3, pp. 291–298, 1992.

[37] J. Wilting, B. Christ, and M. Bokeloh, "A modified chorioallantoic membrane (CAM) assay for qualitative and quantitative study of growth factors. Studies on the effects of carriers, PBS, angiogenin, and bFGF," *Anatomy and Embryology*, vol. 183, no. 3, pp. 259–271, 1991.

[38] C. Balachandran, N. Pazhanivel, T. J. Prabhakar, V. Murugadas, and P. Prabakar, "Avipox virus infection in *Rosella parakeet* (*Platycercus* sp.)," *Journal of Advanced Veterinary and Animal Research*, vol. 2, no. 3, pp. 184–187, 2012.

[39] P. W. Barone and M. S. Strano, "Single walled carbon nanotubes as reporters for the optical detection of glucose," *Journal of Diabetes Science and Technology*, vol. 3, no. 2, pp. 242–252, 2009.

[40] L. Østergaard, A. Tietze, T. Nielsen et al., "The Relationship between tumor blood flow, angiogenesis, tumor hypoxia, and aerobic glycolysis," *Cancer Research*, vol. 73, no. 18, pp. 5618–5624, 2013.

[41] J. D. Murray, G. W. Carlson, K. McLaughlin et al., "Tumor angiogenesis as a prognostic factor in laryngeal cancer," *American Journal of Surgery*, vol. 174, no. 5, pp. 523–526, 1997.

[42] F. Beatrice, R. Cammarota, C. Giordano et al., "Angiogenesis: prognostic significance in laryngeal cancer," *Anticancer Research*, vol. 18, no. 6, pp. 4737–4740, 1998.

[43] K. Kupisz, D. Chibowski, J. Klatka, S. Klonowski, and A. Stepulak, "Tumor angiogenesis in patients with laryngeal cancer," *European Archives of Oto-Rhino-Laryngology*, vol. 256, no. 6, pp. 303–305, 1999.

[44] A. B. Villaret, D. Barbieri, G. Peretti et al., "Angiogenesis and lymphangiogenesis in early-stage laryngeal carcinoma: prognostic implications," *Head & Neck*, vol. 35, no. 8, pp. 1132–1137, 2013.

[45] J. Laitakari, V. Näyhä, and F. Stenbäck, "Size, shape, structure, and direction of angiogenesis in laryngeal tumour development," *Journal of Clinical Pathology*, vol. 57, no. 4, pp. 394–401, 2004.

[46] A. Moscona, "Squamous metaplasia and keratinization of chorionic epithelium of the chick embryo in egg and in culture," *Developmental Biology*, vol. 1, no. 1, pp. 1–23, 1959.

[47] A. Zijlstra, J. Lewis, B. DeGryse, H. Stuhlmann, and J. P. Quigley, "The inhibition of tumor cell intravasation and subsequent metastasis via regulation of *in vivo* tumor cell motility by the tetraspanin CD151," *Cancer Cell*, vol. 13, no. 3, pp. 221–234, 2008.

Hindawi Publishing Corporation
BioMed Research International
Volume 2015, Article ID 497610, 11 pages
http://dx.doi.org/10.1155/2015/497610

Clinical Study

Second Surgery in Insular Low-Grade Gliomas

Tamara Ius,[1] Giada Pauletto,[2] Daniela Cesselli,[3] Miriam Isola,[3] Luca Turella,[4] Riccardo Budai,[2] Giovanna DeMaglio,[5] Roberto Eleopra,[2] Luciano Fadiga,[6,7] Christian Lettieri,[2] Stefano Pizzolitto,[5] Carlo Alberto Beltrami,[3] and Miran Skrap[1]

[1]*Neurosurgery Unit, Department of Neurosciences, Santa Maria della Misericordia University Hospital, Udine, Italy*
[2]*Neurology Unit, Department of Neurosciences, Santa Maria della Misericordia University Hospital, Udine, Italy*
[3]*Department of Medical and Biological Sciences, University of Udine, Udine, Italy*
[4]*Center for Mind/Brain Sciences (CIMeC), University of Trento, Trento, Italy*
[5]*Surgical Pathology Department, Santa Maria della Misericordia University Hospital, Udine, Italy*
[6]*Robotics, Brain and Cognitive Sciences Department, Italian Institute of Technology, Genoa, Italy*
[7]*Section of Human Physiology, University of Ferrara, Ferrara, Italy*

Correspondence should be addressed to Tamara Ius; tamara.ius@gmail.com

Received 15 March 2015; Revised 15 August 2015; Accepted 31 August 2015

Academic Editor: Franco Fulciniti

Background. Given the technical difficulties, a limited number of works have been published on insular gliomas surgery and risk factors for tumor recurrence (TR) are poorly documented. *Objective*. The aim of the study was to determine TR in adult patients with initial diagnosis of insular Low-Grade Gliomas (LGGs) that subsequently underwent second surgery. *Methods*. A consecutive series of 53 patients with insular LGGs was retrospectively reviewed; 23 patients had two operations for TR. *Results*. At the time of second surgery, almost half of the patients had experienced progression into high-grade gliomas (HGGs). Univariate analysis showed that TR is influenced by the following: extent of resection (EOR) ($P < 0.002$), $\Delta VT2T1$ value ($P < 0.001$), histological diagnosis of oligodendroglioma ($P = 0.017$), and mutation of IDH1 ($P = 0.022$). The multivariate analysis showed that EOR at first surgery was the independent predictor for TR ($P < 0.001$). *Conclusions*. In patients with insular LGG the EOR at first surgery represents the major predictive factor for TR. At time of TR, more than 50% of cases had progressed in HGG, raising the question of the oncological management after the first surgery.

1. Introduction

Due to its challenging technical access [1–9] and until the publication of Yaşargil et al. [9], the insula has been considered surgically inaccessible for a long time. Thanks to a better understanding of the insular functional anatomy, several experiences of insular surgery have been reported in the last decades [3, 5, 7, 8, 10–13]. In addition, recent studies, based on the objective evaluation of the Extent of Resection (EOR), show that this latter is associated with increased overall survival (OS) rates and a delayed tumor progression (PFS) [2, 5, 7, 8, 14–16]. The main limiting factor, in LGGs, the achievement of a radical resection is the involvement of eloquent cortical areas and subcortical functional pathways [17–19].

Although surgery is considered the first therapeutic option [2, 5, 7–9, 11], indications for a second operation in case of TR are still poorly documented [20, 21].

The aim of the study was to determine factors influencing the tumor recurrence (TR) in a cohort of adult patients with an initial diagnosis of insular Low-Grade Gliomas (LGGs) that underwent a second surgery, without any adjuvant treatments between surgeries.

2. Methods

2.1. Patient Selection. In the present study, we retrospectively reviewed 53 adult patients with insular LGGs, identifying among them a series of 23 cases who underwent a second

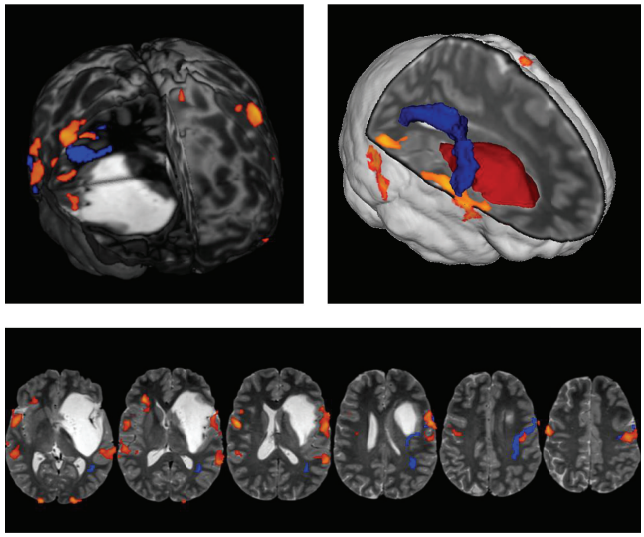

Figure 1: A case of vast left fronto-temporo-insular LGG. Functional MRI/DTI data were overlapped on T2-weighted MRIs and loaded into the Neuro-Navigation system, allowing a better evaluation of the preoperative surgical planning. In the 3D rendering the lesion is represented in red, and the arcuate fasciculus (AF) is in blue, while the orange fMRI spots represent the Broca (anterior spot) and Wernicke area (posterior spot). The functional analysis highlights the cortical areas activated by counting, object naming, and verb generation tasks. The eloquent cortical regions, displaced by the tumor, were easily detected with cortical mapping during surgical procedure. The tumor mass displaces the AF upwards (ACHIEVA 3 T MRI, Philips, Netherlands).

surgery for TR, between January 2000 and September 2013. To analyse the subpopulation with TR and reduce the selection bias, patients were enrolled on the basis of the following inclusion criteria:

(1) Age older than 18 years.

(2) LGGs harboring in the insular lobe.

(3) Two operations during disease evolution.

(4) A period of at least one year between the two operations.

(5) Histological confirmation of infiltrative LGG at first surgery.

(6) Intraoperative mapping at both first and second surgery.

(7) No adjuvant therapy since the first surgery.

The local institution ethics committee on human research approved this study.

2.2. Functional Preoperative Assessment and Surgical Technique. In all cases, high quality 3D T1- and T2-weighted anatomical images as well as functional Magnetic Resonance Imaging (MRI) and diffusion tensor images data were acquired and adopted for the surgical planning and during the surgical procedure itself, after being loaded within a Neuro-Navigation system (Figure 1).

The awake surgery protocol was selected, for both the first and the second surgical procedures, in all cases with lesion harboring on dominant hemisphere, following the methodology previously described by Skrap and colleagues [8].

Moreover, neurophysiological monitoring (MEPs, SEPs, EEG, and ECoG) was employed in all cases following the protocol approved at our institution [14].

2.3. Histological and Molecular Analysis. Tumors were histologically reviewed according to the World Health Organization (WHO) classification for tumors of the central nervous system [22]. Immunohistochemistry and FISH analyses were performed on 4 μm thick formalin-fixed paraffin-embedded slides as previously described [23].

Briefly, primary antibodies against Ki-67, GFAP, p53 (Dako), EGFR (Zymed), and IDH1R132H (Dianova) were detected using EnVision FLEX system (Dako). Ki-67 was scored as percentage of positive nuclei. All other markers were qualitatively evaluated as negative or positive. FISH analysis for 1p36 and 19q13 deletions was performed using dual-color 1p36/1q25 and 19q13/19p13 probes (Vysis). IDH gene status and MGMT promoter methylation were assessed on DNA extracted from formalin-fixed paraffin-embedded tissue (QIAamp DNA Mini Kit, Qiagen). IDH1 and IDH2 gene status was evaluated by pyrosequencing as previously reported [23]. After DNA bisulfite conversion with EpiTect Bisulfite Kit (Qiagen), methylation levels of the MGMT promoter in positions 17–39 of exon 1 were investigated, by PyroMark Q96 CpG MGMT (Qiagen) according to the manufacturers' instructions.

2.4. Outcome Measures and Follow-Up. After surgery, all patients were clinically evaluated at 1, 3, and 6 months. Subsequently, patients were assessed every six months by both clinical examination and MRI.

The TR has been defined as the demonstration of either unequivocal increase in tumor size or detection of gadolinium enhancement (malignant progression) on follow-up imaging.

Seizure outcome was categorized after first surgical procedure, using the Engel Classification (Class I, seizure-free or only auras since surgery; Class II, rare seizures; Class III, meaningful seizure improvement; and Class IV, no seizure improvement or worsening) [24]. Seizure recurrence in seizure-free patients and seizure worsening in those who continued to experience seizure (i.e., increase in seizure frequency or significant changing in ictal semiology) were considered as a warning sign prompting to a clinical and neuroradiological follow-up.

2.5. Volumetric Analysis. All pre- and postoperative tumoral segmentations were performed manually across all MRI slices with the OSIRIX software tool [25] to measure tumor volumes (cm^3) on the basis of T2 axial slices, as previously described [8, 14]. The extent of glioma removal was evaluated by using MRI images acquired six months after surgery. The EOR was calculated as follows: (preoperative tumor volume − postoperative tumor volume)/preoperative tumor volume

[16]. Preoperative $\Delta VT2T1$ value, a preoperative estimation of the difference between tumor volumes on T2-weighted MRI images and on postcontrast T1-weighted MRI images, was also assessed to define the tumor growing pattern, following the methodological procedure described by Skrap et al. [8].

2.6. Statistical Analysis. Characteristics of the study population are described using means ± s.d. or median and range for continuous variables and percentages for categorical variables. Data were tested for normal distribution using the Kolmogorov-Smirnov test. t-test or Mann-Whitney test, as appropriate, was used to compare continuous variables. For categorical variables, cross-tabulations were generated and a chi-square or Fisher exact test was used to compare distributions. To describe the time to TR (time between the first and the second surgeries), the Kaplan-Meier approach was used. Patients with not known progression whether malignant or otherwise were censored at the last scan date available. Univariate and Multivariate Cox regression model was used to explore the predictors associated with TR and, consequently, with a second surgery. In Univariate analysis, variables considered as possible predictors of TR were as follows: age, gender, tumor side, preoperative tumor volume, tumor histological subtype, EOR, $\Delta VT2T1$ value, histological subtype, and molecular markers (Ki-67 (Mib1), GFAP, EGFR, p53, and 1p/19q codeletion; MGMT *promoter methylation*, IDH1-IDH2 mutational status). Considering the small simple size, Multivariate stepwise backward analyses included all variables significant at $P \leq 0.05$ in Univariate analysis [26]. Results are presented as hazard ratios (HR) and 95% confidence intervals (95% CI). Parametric or nonparametric correlation analyses, as appropriate, were used to explore possible association between TR and seizures after the first surgical procedure. All analyses were conducted with Stata/SE 12.0 for Microsoft Windows. All 2-tailed statistical significance levels were set at $P < 0.05$.

3. Results

Baseline demographic, clinical, radiological, and histopathological characteristics of the study population, at the time of first and second surgery, are summarized in Tables 1 and 2, respectively.

3.1. Clinical, Radiological, and Histological Data at First Surgical Procedure. The median time between the diagnosis and the first operation was 3.2 months (range 0–11 months). No patient received adjuvant treatment before the first surgical procedure. Preoperative neurological examination was normal in all cases, but all patients were affected by tumor-related epilepsy and required antiepileptic treatment. Before surgery all patients were drug-resistant, according to the ILAE definition [27].

During surgery, when direct electrical stimulation, at subcortical level, did not elicit any functional response, resection continued following the information provided by guided navigation system which remains indicative in subcortical areas. Neuropathological examination resulted in WHO grade II gliomas in all cases. Worsening of the neurological status after surgery was observed in 15 patients. At the six-month follow-up examination, the neurological conditions of all but one patient improved and returned to the initial level. Concerning seizure outcome, 75.5% of patients achieved satisfactory postoperative seizure control (Engel Classes I-II) 6 months after surgery.

3.2. Clinical, Radiological, and Pathological Data at the Second Surgical Procedure. A second surgery was performed in 23 patients. The median time between surgeries was 81 months (range 12–144 months). At the time of the second operation, 11 patients, who were seizure-free after the first surgery, had a relapse of unprovoked seizures. Seven patients, who were in Engel class II after the first operation, showed increased seizure frequency and/or ictal semiology worsening. In the remaining 6 cases, tumor relapse was identified on the basis of the MRI follow-up. Postoperative seizure recurrence and worsening were found to be associated with TR (Fisher $P < 0.001$). Considering MRI characteristics, 11 cases showed contrast enhancement, while in 12 cases an increased tumor size was observed through radiological follow-up on T2-weighted images. All tumor recurrences were local.

The preoperative neurological examination was normal in all cases. During surgery, motor function was detected in all cases at both cortical and subcortical level whenever necessary due to the extension of the tumor. No changes in intraoperative MEPs recordings were observed during the whole surgical procedure. Regarding language, we were able to obtain a positive mapping in 85% and 25% of cases at cortical and subcortical level, respectively.

New deficits during the immediate postoperative phase were recorded in 8 cases. At the six-month follow-up examination, the neurological conditions of all but one patient improved and returned to the preoperative level. Histopathological examination showed a progression of the glioma to grade III or IV according to WHO in 17 cases.

Comparison between preoperative MRI enhancement and pathological examination showed that enhancement occurred in 13 out of 17 patients with tumor dedifferentiation. The association between contrast enhancement and the progression to grades III and IV was statistically significant (Fisher $P = 0.027$). Postoperative chemotherapy and radiotherapy were administered in all cases with a diagnosis of glioma grade III or IV.

3.3. Volumetric Analysis. The median preoperative tumor volume at first surgery was 76 cm^3 (range 5–174 cm^3) on T2-weighted MRI images, while the median postoperative residual tumor volume, computed on postoperative T2-weighted MRI images, was 12 cm^3 (range 4–85 cm^3). Notably, in almost half of the patients at the first surgery, the EOR was higher than 90% (Figure 2). The median extent of tumor volume resection was 83% (range 54–100%).

In order to evaluate the role of a diffuse tumor growth pattern on tumor recurrence, preoperative $\Delta VT2T1$ value was computed in all cases. For this purpose, the study population was divided into two subgroups (subgroup A (37

Table 1: Demographic, clinical, neuroradiological, and pathological data at first surgery.

Parameter	Value
Number of patients	53
Sex	
Female	23 (43.40%)
Male	30 (56.60%)
Mean age (yrs)	38 (range 19–69)
Tumor side	
Left	36 (67.92%)
Right	17 (32.08%)
Median preoperative T2 tumoral volume in cm^3 (range)	76.33 (range 5–174)
Median preoperative $\Delta VT2T1$ *value* in cm^3 (range)	23.13 (range 1–112)
$\Delta VT2T1$ category	
$<30\ cm^3$	37 (69.81%)
$\geq 30\ cm^3$	16 (30.19%)
Intraoperative protocol	
Awake surgery	41 (77.36%)
General anesthesia	12 (22.64%)
Cortical mapping	
Speech arrest and motor function orbicularis oris	All 41 cases with lesion involving the dominant hemisphere
Slurred speech or dysarthria	26 (49%)
Anomia	26 (49%)
Subcortical mapping	
Identification of corticospinal tract as posterior edge of resection	All cases
Identification of subcortical language pathways	Positive sites were detected in 24 cases (45.3%)
Neurophysiological data	
Reversible reduction of MEPs amplitude	7 out of 10 patients, who developed postoperative transient motor deficit
Irreversible MEPs loss	In 1 patient who showed, after surgery, a permanent motor deficit
Median EOR in % (range)	82.98 (range 54–100)
EOR category	
≥90%	22 (41.51%)
70–89%	23 (43.40%)
<70%	8 (15.09%)
Immediate postoperative clinical findings	
No deficits	37 (69.81%)
Neurological deficits	15 (30.19%)
Motor deficits	9 (16.98%)
Speech disorders	6 (13.21%)
Clinical outcome 6 months after surgery	
No deficits	52 (98.11%)
Neurological deficits	1 (1.89%)
Postoperative Engel Class 6 months after surgery	
I	36 (67.92%)
II	4 (7.55%)
III	8 (15.10%)
IV	5 (9.43%)
Histological diagnosis	
Fibrillary astrocytoma	31 (58.5%)
Oligodendroglioma	6 (11.3%)
Oligoastrocytoma	16 (30.2%)
Molecular profile	
Mib1-Ki-67 expression	3.5% (range 1–5%)
1p/19q codeletion presence	13 (25%)
P53 expression	33 (62.26%)
IDH1 mutation	45 (85%)
MGMT promoter methylation	39 (73.58%)

Table 2: Summary of characteristics at tumor recurrence in the subgroup of patients who underwent a second surgery.

Parameter	Value
Number of patients	23
Sex	
Female	8 (34.78%)
Male	15 (65.22%)
Mean age (yrs)	42 (range 25–54)
Tumor side	
Left	15 (65.22%)
Right	8 (34.78%)
Median time to tumor recurrence	81 months (14–124)
Seizures relapse at second surgery	11 (47.83%)
New contrast enhancement before second surgery	11 (47.83%)
Intraoperative protocol	
Awake surgery	16 (69.57%)
General anesthesia	7 (30.43%)
Immediate postoperative findings	
No deficits	15 (65.22%)
Neurological deficits	08 (34.78%)
Motor deficits	4 (17.39%)
Speech disorders	3 (13.04%)
Visual field disorders	1 (4.35%)
Clinical outcome 6 months after surgery	
No deficits	22 (95.65%)
Neurological deficits	1 (4.35%)
Histological data	
LGGs (WHO II)	6 (26.09%)
Anaplastic gliomas (WHO III)	7 (30.43%)
Glioblastomas (WHO IV)	10 (43.48%)
Mib1-Ki-67 expression	16.5% (range 2–70%)

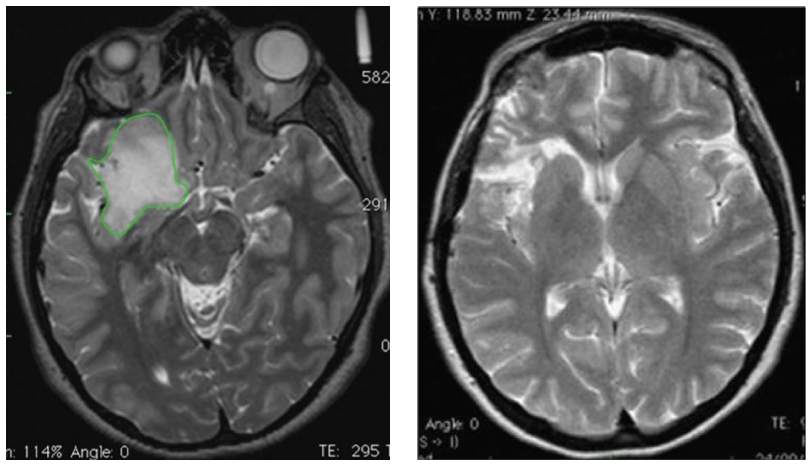

(a) (b)

Figure 2: A case of right insular oligoastrocytoma. (a) The preoperative tumor volume computed on postcontrast T2-weighted MRI was 53 cm^3 (axial slices). The green line represents the area of the tumor before the first surgery. Tumor volume was computed with OSIRIX software. (b) Postoperative tumor residue computed on T2-weighted MRI showed a tumor residual volume of 3 cm^3 (axial slices). The extent of the tumor volume resection, computed on a T2-weighted MRI sequences, was 94%.

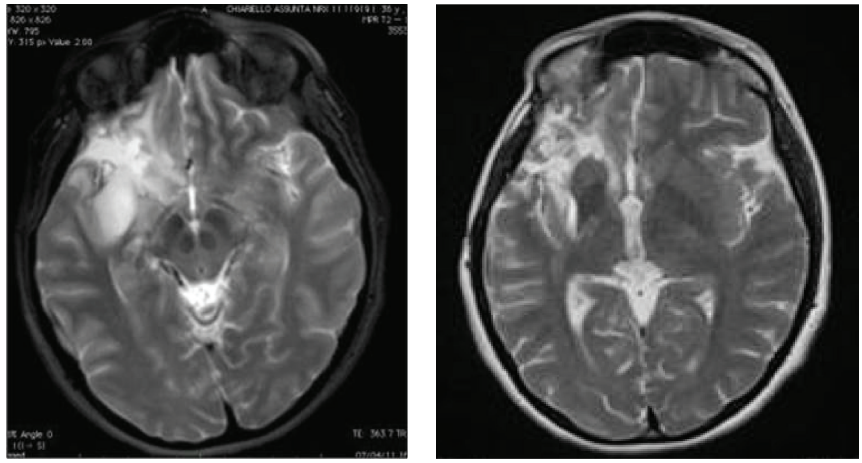

(a) (b)

Figure 3: (a) Showing a TR 62 months after the first surgery. The patient did not receive any adjuvant therapy since the first surgery. The volumetric data at first surgery are shown in Figure 2. At second surgery the preoperative tumor volume computed on T2-weighted MRI was 37 cm^3. Volumetric analysis of postoperative tumor residue computed on T2-weighted MRI showed a tumor residual volume of 4 cm^3 (axial slices), which has grown mainly in the previous cavity (b). The extent of the tumor volume resection, computed on a T2-weighted MRI sequences, was 91%.

cases): patients with $\Delta VT2T1$ value $< 30\,cm^3$ and subgroup B (15 cases): patients with $\Delta VT2T1$ value $\geq 30\,cm^3$). At second surgery, the median preoperative tumor volume, computed on T2-weighted images, was $40\,cm^3$ (range 18–$95\,cm^3$) (Figure 3). The median extent of tumor volume resection, computed on T2-weighted images, was 82% (range 60–100%). Contrast enhancement, observed before the second operation, was totally removed in all 11 cases.

3.4. Risk Factors for Tumor Recurrence. TR was identified in 23 patients. Univariate analysis results are summarized in Table 3. The most important predictor for TR event was the EOR achieved at the first procedure. Patients with TR had a mean EOR of 77.64%; conversely patients without TR had a mean EOR of 90.14% (Mann-Whitney test, $z + -4.99$; $P < 0.0001$). Besides a lower EOR at first surgery (Figure 4(a)), an increase in preoperative $\Delta VT2T1$ value at the diagnosis (Figure 4(b)), as well as the diagnosis of fibrillary astrocytoma (Figure 4(c)), was associated with higher risk to develop TR. Furthermore, the TR event was decreased for those patients with IDH1 mutation (Figure 4(d)), while the presence of 1p/19q codeletion status was associated with the trend to have a lower risk of TR. In the final model, Cox analysis showed that EOR was the strongest independent predictor for TR (Table 4).

4. Discussion

Increasing evidence supports the association between EOR, prolonged OS, and delaying tumor progression [14, 16, 24, 28–40], even for patients with insular LGGs [2, 5, 7–9, 12]. However radical surgery in these cases still remains a critical point, due to insular complex anatomy and functional relationships [1, 2, 8, 18]. Imaging follow-up shows that the residual tumor systematically exhibits a spontaneous and continuous growth, with an inherent risk of anaplastic transformation over the time [18, 41]. While the benefits of an extensive initial resection have been widely demonstrated, the best management of residual tumor still represents an open question [37, 42]. Only two recent investigations analyzed the role of second surgery in case of TR [20, 21] and documented safety and effectiveness of the second surgical procedure in patients with insular LGGs.

4.1. Neurological Deficits and Functional Outcome. The major limitation in achieving a radical resection in LGGs surgery is represented by their attitude to infiltrate the subcortical functional pathways [8, 14, 18]. Thus it is a widespread opinion that a second surgery would lead only to an increased risk of new neurological deficits. For the first time Schmidt et al. [21] provided clinical evidence of the safety of a second surgery in 40 patients.

Martino and coworkers analyzed the clinical outcomes of 19 patients with recurrent LGGs in eloquent areas [20], strengthening the concept of possible functional reshaping occurrence after the first surgical procedure [20, 43–45]. In line with these findings, our postoperative neurological results showed that a second surgery is a safe and effective procedure, even for recurrent insular LGGs.

Another possible reason for the positive outcome after a second surgery may be the smaller tumor volume at relapse. This is coherent with the concept of the "*multistage surgical approach*" for LGGs, previously described by Robles et al. [44]. Our investigation also highlights that seizure recurrence in patients who were seizure-free after the first surgery is associated with tumor progression, as previously described by Chang et al. [46].

Table 3: Univariate analysis of clinical and volumetric tumor data and histological and molecular parameters with tumor recurrence in patients with insular LGGs.

Factor	Tumor recurrence		
	HR	95% CI	*P*
Age (modelled as continuous variable)	1.009	0.973–1.047	0.608
Sex			
Male	1		
Female	1.368	0.595–3.415	0.460
Tumor site			
Left	1		
Right	0.886	0.359–2.183	0.792
Preoperative T2 tumor volume cm^3 (modelled as continuous variable)	1.005	0.994–1.016	0.399
Tumor subtype			
Fibrillary astrocytoma	1		
Oligoastrocytoma	0.509	0.195–1.324	0.166
Oligodendroglioma	0.081	0.011–0.643	**0.017**
% EOR (modelled as continuous variable)	0.932	0.899–0.965	**0.000**
% EOR			
≥90	1		
70–89	2.792	0.938–7.931	**0.052**
≤69	8.936	2.302–34.687	**0.002**
Δ*VT2T1* (modelled as continuous variable)	1.045	1.022–1.068	**0.000**
Δ*VT2T1*			
<30 cm^3	1		
≥30 cm^3	2.950	1.243–7.001	**0.014**
Mib1-Ki-67 (modelled as continuous variable)	0.931	0.722–1.201	0.585
1p/19q codeletion *Presence versus absence*	0.288	0.082–1.003	**0.051**
P53 mutation (modelled as continuous variable)	1.006	0.994–1.018	**0.317**
EGFR (modelled as continuous variable)	0.995	0.983–1.008	0.946
GFAP (modelled as continuous variable)	1.007	0.993–1.021	0.323
IDH1 *Mutation versus no mutation*	0.383	0.168–0.872	**0.022**
MGMT *Promoter methylation versus no promoter methylation*	0.912	0.375–2.215	0.840

HR, hazard ratio; CI, confidence interval; EOR, extent of surgical resection; Δ*VT2T1*, volumetric difference between preoperative tumor volumes on T2- and T1-weighted MRI images.
Boldfacing represents statistical significance values ($P < 0.05$) obtained from two-sided tests (Cox regression).

4.2. Surgical Considerations. The overlap of fMRI/DTI data on the T1/T2 3D MRI images in the Neuro-Navigation system is particularly helpful at second surgery, because anatomy with conventional landmarks and functional structures may be significantly modified [8].

Moreover, intraoperative image guidance may also provide critical information during the resection of tumors with a consistency similar to normal brain tissue, by delineating T2-weighted images margins [47]. For this reason, MEPs monitoring was particularly helpful in preventing the direct

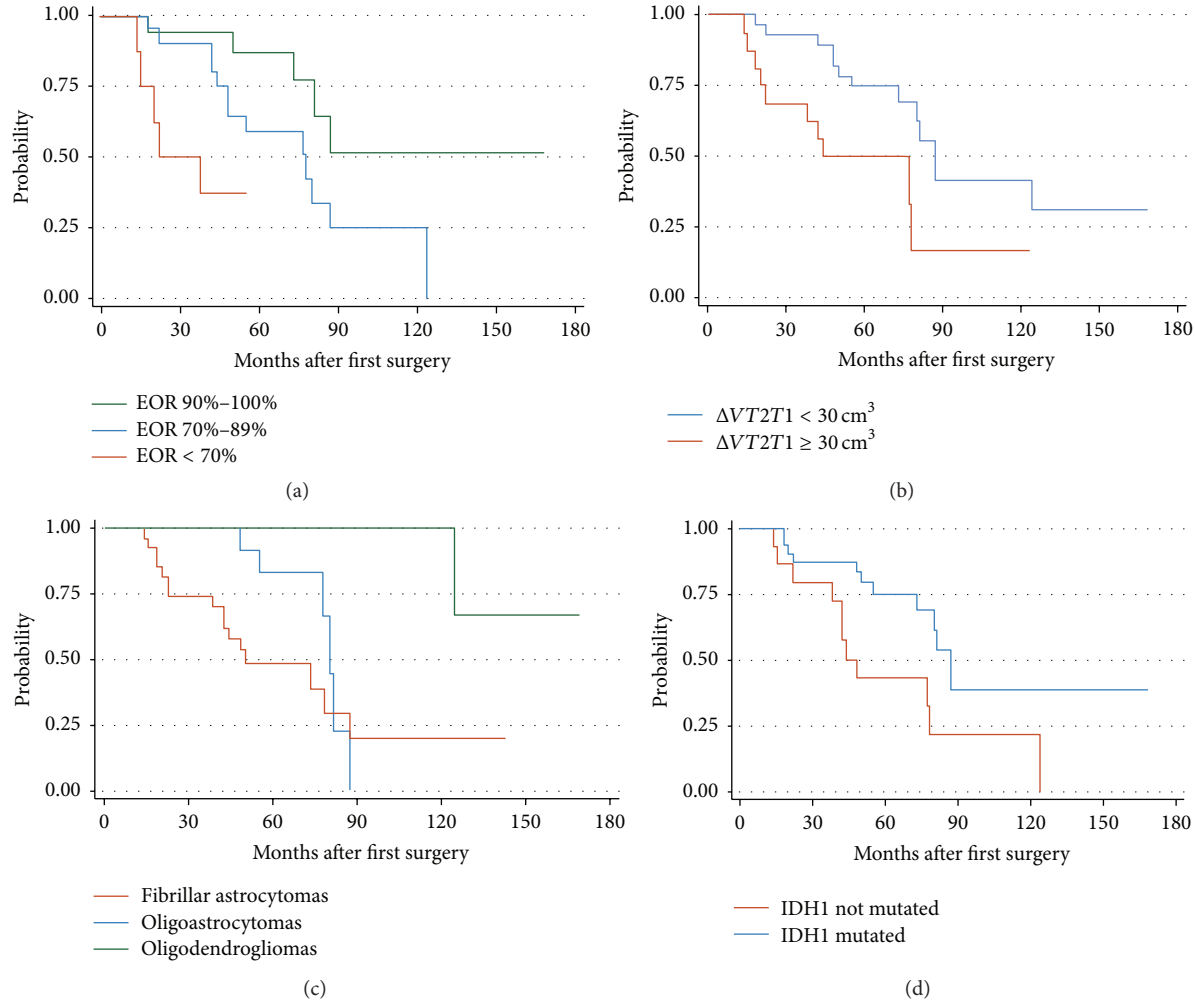

Figure 4: Kaplan-Meier curves revealing TR likelihood in patients with insular Low-Grade Gliomas, stratified by EOR (a), Δ*VT2T1* value (b), histological subtype (c), and IDH1 mutational status (d). Patients with EOR ≥ 90%, Δ*VT2T1* value < 30 cm^3, diagnosis of oligodendroglioma, and the presence of IDH1 mutation showed significantly lower likelihood of TR after first surgery.

Table 4: Variable independently associated with tumor recurrence after surgical resection of insular LGGs in a multivariate proportional hazards analysis (Cox model). In the final model, the EOR remained the strongest independent significant predictor of TR after first surgery for insular LGG.

Factor	Tumor progression		
	HR	95% CI	*P*
% EOR (modelled as continuous variable)	0.930	0.895–0.967	**0.001**

EOR = extent of surgical resection.

injury to the posterior limb of the internal capsule and the superior limit towards the corona radiate [48, 49]. Indeed, both structures have been always identified at first and second surgical procedure. On the contrary, subcortical language pathways have been detected in 46% and 25% of cases, at first surgery and second surgery, respectively. Even so, none of our patients developed permanent severe language deficit, supporting the hypothesis of functional reshaping [2, 20, 45, 50, 51]. From a strictly surgical point of view, there are some technical key points to take into consideration at second surgery. At recurrence, there is no endocranic hypertension. Tumor recurrence volume is smaller than the volume at first surgery and the cavity left by the previous operation allows a larger surgical field. The recurrent mass of tumor tissue mainly regrows from the walls of the previous resection into the cavity. We have noticed, also, a better definition between the healthy parenchyma and the tumor tissue, which is softer and, consequently, easier to remove. Moreover, at second surgery, the risk of damaging the vascular structures is much lower, because dissection of the middle cerebral artery (MCA) and its branches has already been performed during the first surgical procedure.

The only difficulty of second surgery is represented by the adhesions. They may cause pain during the opening; moreover, adhesions between *dura mater* and cortex, on the dominant side, may represent a risk of damage to the cortical

language areas. In conclusion, the newly infiltrated deep tumoral tissue is not resected if it has been shown to still be functional based on brain mapping results.

4.3. Risk Factors for Tumor Progression. The idea of performing a new procedure during regrowth of LGGs, before anaplastic transformation, has been proposed in order to obtain a greater impact on survival [21, 32, 44, 52]. Thus, we tried to identify factors that could provide an early identification of those patients with higher possibility to develop TR. Our findings indicated that the time to TR, even among insular LGGs, is longer in patients who underwent wider resections, as previously demonstrated.

These results support the idea that tumors with larger residual postoperative volume may have an inherently faster growth; therefore, they may recur earlier in the setting of a subtotal resection [15, 16]. Moreover this investigation confirmed the data we previously reported about the role of $\Delta VT2T1$ value on TR: patients with preoperative $\Delta VT2T1$ value more than 30 cm^3 have an earlier TR (P value = 0.001). In fact this value reflects a lower possibility to obtain a higher EOR.

McGirt et al. showed that patients with oligodendroglioma and oligoastrocytoma have a better prognosis compared to those with fibrillary astrocytoma [32]. To support this result we separated these histological subtypes confirming that oligodendrogliomas have more benign courses [8, 53, 54].

Regarding the molecular analysis, recent data demonstrated that LGGs display a variety of molecular alterations that may have predictive or prognostic value [55, 56]. The molecular data pointed out that the risk of TR was significantly reduced in the presence of IDH1 mutation, as previously demonstrated by Gozé et al. [56, 57], while the presence of 1p/19q codeletion status was associated with a lower TR risk trend. The prognostic value of IDH1/IDH2 mutations is more controversial. Otherwise 1p/19q codeletion status in LGGs has been widely demonstrated to be associated with a favorable outcome whatever the endpoint: overall survival, progression-free survival, or spontaneous tumor growth velocity [37, 53, 56, 58]. Furthermore, the molecular analysis evidenced that Ki-67 value, as well as p53, GFAP, EGFR, and MGMT status, does not influence the risk for TR after the first surgical procedure, suggesting that other molecular markers should be selected for early identification of patients with a major risk of TR [23]. In closing, the Multivariate analysis highlighted that the only independent factor associated with TR is represented by EOR at first surgery, confirming the findings reported in the literature [5, 8, 14, 24].

As far as the methodological procedure is concerned, the present investigation has potential limitations. First, it is a retrospective study; thus it is limited in nature. Patients with recurrence insular LGGs that are suitable for second surgery are *per se* highly selected. Thus, the number of our samples is limited, but, if we consider the papers, mentioning insular second surgery [2, 5, 7, 12], the overall number of patients is 32; thus our study population in a singular institution (23 patients) is not considerably small and it is statistically sufficient to draw some preliminary considerations, which need to be confirmed by enlarging the case study. Moreover, insular surgery is rare at first diagnosis and even rarer at second surgery, so it is not easy to find large population in literature. In any case, it is unlikely that a prospective, randomized study will be designed to address these issues; thus, we believe retrospective, matched studies or prospective observational trials may be a more practical solution, as previously described [15]. Our findings should be validated in a wider series, using multi-institutional cohort to create a potential model able to stratify the risk of TR after the first surgery. In this way, it would be possible to anticipate adjuvant postoperative treatments, also in patients with a diagnosis of pure LGG.

The timing of second surgery has not been well defined yet. Anyway, as previously remarked by Martino et al, it is better to "overindicate" an early second surgery than performing a late surgery when the tumor has already transformed into high-grade gliomas, especially in consideration of the low morbidity profile associated with reoperation [20].

5. Conclusions

In insular LGGs patients, the EOR at first surgery represents the major predictive factor for TR. Further molecular analysis will be necessary to better stratify patients in terms of risk for TR, thus identifying patients that could benefit from an early adjuvant treatment after the first surgical procedure.

Abbreviations

DES: Direct electrical stimulation
ECoG: Electrocorticography
EEG: Electroencephalography
EOR: Extent of Resection
DICOM: Digital Imaging and Communications in Medicine (standard)
DTI: Diffusion tensor imaging
fMRI: Functional MRI
KPS: Karnofsky Performance Scale
IES: Intraoperative electrical stimulation
LGGs: Low-Grade Gliomas
MEPs: Motor evoked potentials
MRI: Magnetic Resonance Imaging
SEP: Somatosensory evoked potentials
TR: Tumor recurrence
$\Delta VT2T1$: Volumetric difference between preoperative tumor volumes on T2- and T1-weighted MRI images.

Disclosure

The founders had no role in study design, data collection and analysis, decision to publish, or preparation of the paper.

Conflict of Interests

The authors attest to have no conflict of interests concerning the materials or methods used in this study or the findings specified in this paper.

Authors' Contribution

Authors' contribution to the study and paper preparation includes the following: conception and design: Skrap and Ius; acquisition of data: Ius; analysis and interpretation of data: Ius, Isola, and Skrap; drafting the paper: all authors; critically revising the paper: all authors.

Acknowledgments

The authors thank Programma per la Cooperazione Transfrontaliera Italia-Slovenia 2007–2013 entitled "identificazione di nuovi marcatori di cellule staminali tumorali a scopo diagnostico e terapeutico." Additional thanks are due to Gabriele Valiante and Roberto Canesin for technical support.

References

[1] J. R. Augustine, "Circuitry and functional aspects of the insular lobe in primates including humans," *Brain Research Reviews*, vol. 22, no. 3, pp. 229–244, 1996.

[2] H. Duffau, "A personal consecutive series of surgically treated 51 cases of insular WHO Grade II glioma: advances and limitations," *Journal of Neurosurgery*, vol. 110, no. 4, pp. 696–708, 2009.

[3] U. Ebeling and K. Kothbauer, "Circumscribed low grade astrocytomas in the dominant opercular and insular region: a pilot study," *Acta Neurochirurgica*, vol. 132, no. 1–3, pp. 66–74, 1995.

[4] M.-M. Mesulam and E. J. Mufson, "The insula of Reil in man and monkey: architectonics, connectivity, and function," in *Association and Auditory Cortices*, vol. 4 of *Cerebral Cortex*, pp. 179–226, Springer, New York, NY, USA, 1985.

[5] N. Sanai, M.-Y. Polley, and M. S. Berger, "Insular glioma resection: assessment of patient morbidity, survival, and tumor progression—clinical article," *Journal of Neurosurgery*, vol. 112, no. 1, pp. 1–9, 2010.

[6] B. P. Shelley and M. R. Trimble, "The insular lobe of reil-its anatamico-functional, behavioural and neuropsychiatric attributes in humans-a review," *World Journal of Biological Psychiatry*, vol. 5, no. 4, pp. 176–200, 2004.

[7] M. Simon, G. Neuloh, M. von Lehe, B. Meyer, and J. Schramm, "Insular gliomas: the case for surgical management," *Journal of Neurosurgery*, vol. 110, no. 4, pp. 685–695, 2009.

[8] M. Skrap, M. Mondani, B. Tomasino et al., "Surgery of insular nonenhancing gliomas: volumetric analysis of tumoral resection, clinical outcome, and survival in a consecutive series of 66 cases," *Neurosurgery*, vol. 70, no. 5, pp. 1081–1093, 2012.

[9] M. G. Yaşargil, K. von Ammon, E. Cavazos, T. Doczi, J. D. Reeves, and P. Roth, "Tumours of the limbic and paralimbic systems," *Acta Neurochirurgica*, vol. 118, no. 1-2, pp. 40–52, 1992.

[10] H. Duffau, L. Capelle, M. Lopes, T. Faillot, J.-P. Sichez, and D. Fohanno, "The insular lobe: physiopathological and surgical considerations," *Neurosurgery*, vol. 47, no. 4, pp. 801–810, 2000.

[11] F. F. Lang, N. E. Olansen, F. DeMonte et al., "Surgical resection of intrinsic insular tumors: complication avoidance," *Journal of Neurosurgery*, vol. 95, no. 4, pp. 638–650, 2001.

[12] V. Vanaclocha, N. Sáiz-Sapena, and C. García-Casasola, "Surgical treatment of insular gliomas," *Acta Neurochirurgica*, vol. 139, no. 12, pp. 1126–1135, 1997.

[13] J. Zentner, B. Meyer, A. Stangl, and J. Schramm, "Intrinsic tumors of the insula: a prospective surgical study of 30 patients," *Journal of Neurosurgery*, vol. 85, no. 2, pp. 263–271, 1996.

[14] T. Ius, M. Isola, R. Budai et al., "Low-grade glioma surgery in eloquent areas: Volumetric analysis of extent of resection and its impact on overall survival. A single-institution experience in 190 patients—clinical article," *Journal of Neurosurgery*, vol. 117, no. 6, pp. 1039–1052, 2012.

[15] N. Sanai and M. S. Berger, "Glioma extent of resection and its impact on patient outcome," *Neurosurgery*, vol. 62, no. 4, pp. 753–766, 2008.

[16] J. S. Smith, E. F. Chang, K. R. Lamborn et al., "Role of extent of resection in the long-term outcome of low-grade hemispheric gliomas," *Journal of Clinical Oncology*, vol. 26, no. 8, pp. 1338–1345, 2008.

[17] H. Duffau and L. Capelle, "Preferential brain locations of low-grade gliomas," *Cancer*, vol. 100, no. 12, pp. 2622–2626, 2004.

[18] E. Mandonnet, L. Capelle, and H. Duffau, "Extension of paralimbic low grade gliomas: toward an anatomical classification based on white matter invasion patterns," *Journal of Neuro-Oncology*, vol. 78, no. 2, pp. 179–185, 2006.

[19] N. Sanai, Z. Mirzadeh, and M. S. Berger, "Functional outcome after language mapping for glioma resection," *The New England Journal of Medicine*, vol. 358, no. 1, pp. 18–27, 2008.

[20] J. Martino, L. Taillandier, S. Moritz-Gasser, P. Gatignol, and H. Duffau, "Re-operation is a safe and effective therapeutic strategy in recurrent WHO grade II gliomas within eloquent areas," *Acta Neurochirurgica*, vol. 151, no. 5, pp. 427–436, 2009.

[21] M. H. Schmidt, M. S. Berger, K. R. Lamborn et al., "Repeated operations for infiltrative low-grade gliomas without intervening therapy," *Journal of Neurosurgery*, vol. 98, no. 6, pp. 1165–1169, 2003.

[22] D. N. Louis, H. Ohgaki, O. D. Wiestler et al., "The 2007 WHO classification of tumours of the central nervous system," *Acta Neuropathologica*, vol. 114, no. 2, pp. 97–109, 2007.

[23] E. Bourkoula, D. Mangoni, T. Ius et al., "Glioma-associated stem cells: a novel class of tumor-supporting cells able to predict prognosis of human low-grade gliomas," *Stem Cells*, vol. 32, no. 5, pp. 1239–1253, 2014.

[24] L. Capelle, D. Fontaine, E. Mandonnet et al., "Spontaneous and therapeutic prognostic factors in adult hemispheric World Health Organization Grade II gliomas: a series of 1097 cases," *Journal of Neurosurgery*, vol. 118, no. 6, pp. 1157–1168, 2013.

[25] A. Rosset, L. Spadola, and O. Ratib, "OsiriX: an open-source software for navigating in multi-dimensional DICOM images," *Journal of Digital Imaging*, vol. 17, no. 3, pp. 205–216, 2004.

[26] E. W. Steyerberg, *Clinical Prediction Models: A Practical Approach to Development, Validation, and Updating*, Springer, New York, NY, USA, 2009.

[27] P. Kwan, A. Arzimanoglou, A. T. Berg et al., "Definition of drug resistant epilepsy: consensus proposal by the ad hoc Task Force of the ILAE Commission on Therapeutic Strategies," *Epilepsia*, vol. 51, no. 6, pp. 1069–1077, 2010.

[28] A. Rezvan, D. Christine, H. Christian et al., "Long-term outcome and survival of surgically treated supratentorial low-grade glioma in adult patients," *Acta Neurochirurgica*, vol. 151, no. 11, pp. 1359–1365, 2009.

[29] J. T. Grier and T. Batchelor, "Low-grade gliomas in adults," *Oncologist*, vol. 11, no. 6, pp. 681–693, 2006.

[30] T. B. Johannesen, F. Langmark, and K. Lote, "Progress in long-term survival in adult patients with supratentorial low-grade

gliomas: a population-based study of 993 patients in whom tumors were diagnosed between 1970 and 1993," *Journal of Neurosurgery*, vol. 99, no. 5, pp. 854–862, 2003.

[31] C. Leighton, B. Fisher, G. Bauman et al., "Supratentorial low-grade glioma in adults: an analysis of prognostic factors and timing of radiation," *Journal of Clinical Oncology*, vol. 15, no. 4, pp. 1294–1301, 1997.

[32] M. J. McGirt, K. L. Chaichana, F. J. Attenello et al., "Extent of surgical resection is independently associated with survival in patients with hemispheric infiltrating low-grade gliomas," *Neurosurgery*, vol. 63, no. 4, pp. 700–707, 2008.

[33] M. Nakamura, N. Konishi, S. Tsunoda et al., "Analysis of prognostic and survival factors related to treatment of low-grade astrocytomas in adults," *Oncology*, vol. 58, no. 2, pp. 108–116, 2000.

[34] C. A. North, R. B. North, J. A. Epstein, S. Piantadosi, and M. D. Wharam, "Low-grade cerebral astrocytomas. Survival and quality of life after radiation therapy," *Cancer*, vol. 66, no. 1, pp. 6–14, 1990.

[35] J. H. Philippon, S. H. Clemenceau, F. H. Fauchon, J. F. Foncin, R. A. Morantz, and J. M. Piepmeier, "Supratentorial low-grade astrocytomas in adults," *Neurosurgery*, vol. 32, no. 4, pp. 554–559, 1993.

[36] B. Rajan, D. Pickuth, S. Ashley et al., "The management of histologically unverified presumed cerebral gliomas with radiotherapy," *International Journal of Radiation Oncology, Biology, Physics*, vol. 28, no. 2, pp. 405–413, 1994.

[37] N. Sanai, S. Chang, and M. S. Berger, "Low-grade gliomas in adults," *Journal of Neurosurgery*, vol. 115, no. 5, pp. 948–965, 2011.

[38] J. S. Smith, S. Cha, M. C. Mayo et al., "Serial diffusion-weighted magnetic resonance imaging in cases of glioma: distinguishing tumor recurrence from postresection injury," *Journal of Neurosurgery*, vol. 103, no. 3, pp. 428–438, 2005.

[39] S.-A. Yeh, J.-T. Ho, C.-C. Lui, Y.-J. Huang, C.-Y. Hsiung, and E.-Y. Huang, "Treatment outcomes and prognostic factors in patients with supratentorial low-grade gliomas," *British Journal of Radiology*, vol. 78, no. 927, pp. 230–235, 2005.

[40] A. C. Whitton and H. G. G. Bloom, "Low grade glioma of the cerebral hemispheres in adults: a retrospective analysis of 88 cases," *International Journal of Radiation Oncology, Biology, Physics*, vol. 18, no. 4, pp. 783–786, 1990.

[41] J. Pallud, L. Taillandier, L. Capelle et al., "Quantitative morphological magnetic resonance imaging follow-up of low-grade glioma: a plea for systematic measurement of growth rates," *Neurosurgery*, vol. 71, no. 3, pp. 729–739, 2012.

[42] R. Cavaliere, M. B. S. Lopes, and D. Schiff, "Low-grade gliomas: an update on pathology and therapy," *Lancet Neurology*, vol. 4, no. 11, pp. 760–770, 2005.

[43] H. Duffau, P. Gatignol, E. Mandonnet, L. Capelle, and L. Taillandier, "Intraoperative subcortical stimulation mapping of language pathways in a consecutive series of 115 patients with Grade II glioma in the left dominant hemisphere," *Journal of Neurosurgery*, vol. 109, no. 3, pp. 461–471, 2008.

[44] S. G. Robles, P. Gatignol, S. Lehéricy, and H. Duffau, "Long-term brain plasticity allowing multistage surgical approach to World Health Organization Grade II gliomas in eloquent areas," *Journal of Neurosurgery*, vol. 109, no. 4, pp. 615–624, 2008.

[45] T. Ius, E. Angelini, M. Thiebaut de Schotten, E. Mandonnet, and H. Duffau, "Evidence for potentials and limitations of brain plasticity using an atlas of functional resectability of WHO grade II gliomas: towards a 'minimal common brain'," *NeuroImage*, vol. 56, no. 3, pp. 992–1000, 2011.

[46] E. F. Chang, M. B. Potts, G. E. Keles et al., "Seizure characteristics and control following resection in 332 patients with low-grade gliomas," *Journal of Neurosurgery*, vol. 108, no. 2, pp. 227–235, 2008.

[47] G. E. Keles and M. S. Berger, "Advances in neurosurgical technique in the current management of brain tumors," *Seminars in Oncology*, vol. 31, no. 5, pp. 659–665, 2004.

[48] Y. A. Moshel, J. D. S. Marcus, E. C. Parker, and P. J. Kelly, "Resection of insular gliomas: the importance of lenticulostriate artery position—clinical article," *Journal of Neurosurgery*, vol. 109, no. 5, pp. 825–834, 2008.

[49] G. G. Varnavas and W. Grand, "The insular cortex: morphological and vascular anatomic characteristics," *Neurosurgery*, vol. 44, no. 1, pp. 127–138, 1999.

[50] H. Duffau, "Surgery of low-grade gliomas: towards a 'functional neurooncology'," *Current Opinion in Oncology*, vol. 21, no. 6, pp. 543–549, 2009.

[51] H. Duffau, "Introduction. Surgery of gliomas in eloquent areas: from brain hodotopy and plasticity to functional neurooncology," *Neurosurgical Focus*, vol. 28, no. 2, pp. 1–2, 2010.

[52] T. Kılıç, K. Özduman, I. Elmac, A. Sav, and P. M. Necmettin, "Effect of surgery on tumor progression and malignant degeneration in hemispheric diffuse low-grade astrocytomas," *Journal of Clinical Neuroscience*, vol. 9, no. 5, pp. 549–552, 2002.

[53] C. Hartmann, B. Hentschel, M. Tatagiba et al., "Molecular markers in low-grade gliomas: predictive or prognostic?" *Clinical Cancer Research*, vol. 17, no. 13, pp. 4588–4599, 2011.

[54] R. B. Jenkins, H. Blair, K. V. Ballman et al., "A t(1;19)(q10;p10) mediates the combined deletions of 1p and 19q and predicts a better prognosis of patients with oligodendroglioma," *Cancer Research*, vol. 66, no. 20, pp. 9852–9861, 2006.

[55] T. D. Bourne and D. Schiff, "Update on molecular findings, management and outcome in low-grade gliomas," *Nature Reviews Neurology*, vol. 6, no. 12, pp. 695–701, 2010.

[56] C. Gozé, C. Bezzina, E. Gozé et al., "1P19Q loss but not *IDH1* mutations influences WHO grade II gliomas spontaneous growth," *Journal of Neuro-Oncology*, vol. 108, no. 1, pp. 69–75, 2012.

[57] C. Gozé, L. Mansour, V. Rigau, and H. Duffau, "Distinct IDH1/IDH2 mutation profiles in purely insular versus paralimbic WHO Grade II gliomas: laboratory investigation," *Journal of Neurosurgery*, vol. 118, no. 4, pp. 866–872, 2013.

[58] M. Jansen, S. Yip, and D. N. Louis, "Molecular pathology in adult gliomas: diagnostic, prognostic, and predictive markers," *The Lancet Neurology*, vol. 9, no. 7, pp. 717–726, 2010.